

1
2
3
4
5
6
7
8
9
10
11
12
13
14
15
16
17
18
19
20
21
22
23
24

Articulatory Characterization of English Liquid-Final Rimes

Michael Proctor

Department of Linguistics, Macquarie University

Rachel Walker, Caitlin Smith

Department of Linguistics, University of Southern California

Tünde Szalay

Department of Linguistics, Macquarie University

Louis Goldstein, Shrikanth Narayanan

Department of Linguistics, University of Southern California

Abstract

25
26
27
28
29
30
31
32
33
34
35
36
37
38
39
40

Articulation of liquid consonants in onsets and codas by four speakers of General American English was examined using real-time MRI. Midsagittal tongue posture was compared for laterals and rhotics produced in each syllable margin, adjacent to 13 different vowels and diphthongs. Vowel articulation was examined in words without liquids, before each liquid, and after each liquid, to assess the coarticulatory influence of each segment on the others. Overall, nuclear vocalic postures were more influenced by coda rhotics than onset rhotics or laterals in either syllable margin. Laterals exhibited greater temporal and spatial independence between coronal and dorsal gestures. Rhotics were produced with a variety of speaker-specific postures, but were united by a greater degree of coarticulatory resistance to vowel context, patterns consistent with greater coarticulatory influence on adjacent vowels, and less allophonic variation across syllable positions than laterals.

41
42

Keywords: liquid consonant, rhotic, lateral, coarticulation, syllable structure

1. Introduction

43
44
45
46
47
48
49
50
51
52

Liquid consonants in American English exhibit asymmetries with respect to the range of contrasts in co-occurring vowels in the rime. Fewer vowel contrasts are attested before coda rhotics than laterals (Hammond, 1999; Proctor & Walker, 2012). For example, in General American English (Wells, 1982), tense and lax vowel contrasts, such as /i/-/ɪ/ and /eɪ/-/ɛ/, are neutralized before a coda rhotic, as in words like *beer* and *bare*,

53
54

Email address: michael.proctor@mq.edu.au (Michael Proctor)

55
56
57
58
59

Preprint submitted to Journal of Phonetics

August 28, 2019

60 while the same contrasts are maintained before a coda lateral, as in words like *peel* versus *pill* (/i/-/ɪ/) 61
62 and *fail* and *fell* (/eɪ/-/ɛ/). Nonetheless, neutralization of vowel contrasts preceding a coda lateral occurs 63
64 in some varieties of American English, though with weaker effect than that of the rhotic. For example, in 65
66 varieties of Southern American English, the /i/-/ɪ/ contrast is also neutralized before a coda lateral, and 67
68 there is a weaker propensity for merger of the /eɪ/-/ɛ/ contrast in the same context (Labov et al., 2005). 69
70 It is conceivable that these asymmetries are grounded in phonetic differences between laterals and rhotics; 71
72 however, this possibility is difficult to assess given the information available from previous studies. 73
74

75 To the best of our knowledge, lateral and rhotic production has not yet been systematically compared in 76
77 the same speakers, in the full range of vowel contexts and syllable positions of General American English. 78
79 In particular, we lack comprehensive instrumental data on how coda liquids are produced after different 80
81 vowels, allowing a direct comparison of lateral and rhotic behavior in rimes. Data on liquid production 82
83 have also been limited in the scope of coverage provided by some sensing modalities. EPG, EMA, XRMB 84
85 and ultrasound have provided rich data on lingual targets and timing, but each from restricted regions of 86
87 the tongue. Static structural MRI has facilitated a more complete view of the upper airway and lingual 88
89 postures associated with liquid allophones, but has not allowed dynamic characterization of vowel-consonant 90
91 and consonant-vowel coproduction patterns. We address this deficit in this study by making use of the richer 92
93 information afforded by real-time magnetic resonance imaging (rtMRI: Narayanan et al., 2004) about the 94
95 dynamic configuration of the vocal tract. 96
97

98 Despite the foregoing deficit in research on liquid production in General American English, previous 99
100 studies of these consonants in English varieties have yielded an extensive body of work with relevant insights 101
102 on which we build (in overview, see, e.g., Krakow, 1999; Gick, 2003; Gick & Campbell, 2003; Proctor & 103
104 Walker, 2012). Two key articulatory properties that are common to American English liquids emerge from 105
106 these studies. The first is *gestural complexity*. Laterals require temporal and spatial coordination of two 107
108 gestures, which may be loosely characterized as coronal and dorsal (Giles & Moll, 1975; Sproat & Fujimura, 109
110 1993), while rhotics are prototypically produced with three coordinated gestures: labial, anterior lingual, 111
112 and pharyngeal. The second key property is *syllabic positional sensitivity*. Both laterals and rhotics exhibit 113
114 allophonic variation conditioned by their position in the syllable: post-vocalic laterals are typically ‘darker’ 115
116 (produced with a more retracted/lowered tongue body) than their pre-vocalic counterparts (Narayanan 117
118 et al., 1997; Lee-Kim et al., 2013); pre-vocalic /l/ is more labialized and more often retroflexed than its 119
120 post-vocalic and syllabic variants (Uldall, 1958; Delattre & Freeman, 1968; Zawadzki & Kuehn, 1980; Mielke 121
122 et al., 2016). Gestural coordination patterns also differ systematically across these environments for both 123
124 liquids (Sproat & Fujimura, 1993; Browman & Goldstein, 1995a; Gick et al., 2003, 2006; Scobbie & Pouplier, 125
126 2010). Most relevant to our focus on distributions in rimes of General American English is the finding that 127
128 in coda liquids the more posterior lingual gesture begins before the anterior lingual gesture. 129

130 The coupled oscillator model of Articulatory Phonology has been influential in modeling the representa-

119
120
121
122
123
124 tion of multi-gestural liquids with regard to coordination of their articulations within and across segments
125 (Browman & Goldstein, 1986, 1989, 1992; Saltzman et al., 1987; Krakow, 1999; Nam et al., 2009, etc.).
126 This is especially important for coda liquids, where the dorsal or pharyngeal gesture precedes a coronal
127 articulation, and therefore potentially shows greater overlap and interaction with the preceding vowel. An
128 examination of coarticulatory effects can shed light on the nature of the interaction between overlapping
129 and competing articulations. Recasens et al. (1997) and Recasens & Rodríguez (2016, 2017) have found
130 that the coarticulatory dominance of a segment, referring jointly to its resistance to coarticulation from
131 other segments and the aggressiveness of its coarticulatory effect on other segments, depends on a segment's
132 manner and the articulators involved in its formation. For liquid consonants in Catalan, the trill [r] is found
133 to have a higher coarticulatory dominance than the lateral [l] and the flap [ɾ] (Recasens & Rodríguez, 2016).
134 Bladon & Al Bamerni (1976) found that dark [ɫ] exhibits greater coarticulation resistance (a term they
135 coined) than clear [l] in RP English; however, the relative coarticulatory dominance of the lateral and rhotic
136 in American English have not previously been examined.
137

138
139
140
141
142 In the dynamical formal framework of Articulatory Phonology, differences in coarticulatory dominance
143 can be represented by the specified blending strength for a gesture (Saltzman & Munhall, 1989; Fowler &
144 Saltzman, 1993). In this model, when overlap occurs between two gestures that impose conflicting demands
145 on the same articulator, their goal articulatory states are blended, with the outcome being the weighted
146 average of the individual goal articulatory states, based on the specified blending strength of each. Gestures
147 with a higher specified blending strength are expected to exhibit greater coarticulatory dominance, with
148 the potential to induce stronger neutralization effects on other gestures with which they overlap and to
149 show greater resistance to neutralization. Given that greater neutralization of vowel contrasts occurs before
150 coda rhotics than coda laterals in General American English, we hypothesize that the rhotic has a posterior
151 lingual gesture with stronger blending strength than that of the lateral in this dialect. This hypothesis
152 predicts that the rhotic will show less variance in articulation than the lateral across vocalic contexts and
153 syllable positions, owing to the rhotic's hypothesized greater coarticulatory resistance. It also predicts that
154 the articulation of vowels will be more affected in the context of a coda rhotic than a coda lateral, owing to
155 the rhotic's hypothesized greater coarticulatory aggression.
156
157
158
159
160
161

162 *1.1. Goals*

163
164 In summary, the goal of this study is to examine in new detail the articulation of liquid-final rimes in
165 General American English, to shed more light on their shared characteristics and the phonotactic asymme-
166 tries between liquids and preceding vowels. By making use of the richer information about the configuration
167 of the vocal tract provided by rtMRI, we aim in particular to examine the relative coarticulatory dominance
168 of rhotics and laterals on the following points:
169
170

- 171 1. compare the articulation of liquid consonants across a complete range of vowel contexts

- 178
179
180
181
182
183
184 75 2. compare the articulation of liquid consonants in coda position with their onset equivalents
185 3. compare the articulation of vowels produced before coda liquids with vowels unaffected by coarticula-
186 tory influences from adjacent liquid consonants
187
188

189 **2. Material and Methods**
190

191 We examined patterns of liquid consonant production and coarticulation in the midsagittal plane, using
192 80 real-time structural magnetic resonance imaging sequences specially developed to track dynamic configura-
193 tion of the upper airway during speech (Narayanan et al., 2004). This technology offers new insights into
194 liquid consonant production because it images the whole vocal tract, including the tongue body, tongue
195 root and pharynx: regions which have proven difficult to track using other methods, but which provide
196 critical detail about tongue shaping in laterals, rhotics, and vowels, and the coordination of lingual and
197 other gestures.
198
199 85 other gestures.
200

201
202 *2.1. Subjects and Stimuli*

203 Four native speakers of General American English participated in the study, with ages ranging from 23
204 to 28 years (Table 1). Although from geographically diverse backgrounds, all four informants are college-
205 educated L1 speakers raised in the USA who were selected for participation because their accents are not
206 characteristic of any particular region, and because both parents are fluent speakers of American English.
207 90
208 None of the speakers reported abnormal hearing or speaking development or pathologies.
209
210

211 Table 1: **Study Participants – Demographic Details.**

212
213

| ID | GENDER | AGE | BIRTHPLACE |
|----|--------|-----|------------------|
| W1 | Female | 27 | San Clemente, CA |
| W2 | Female | 27 | Babylon, NY |
| W3 | Female | 28 | Brawley, CA |
| M1 | Male | 23 | Baltimore, MD |

214
215
216
217
218
219
220

221
222 *2.2. Experimental Materials*
223

224 Lateral and rhotic approximants were elicited in onset and coda positions in monosyllabic real and
225 nonce words, adjacent to each of the vowels of General American English, subject to phonotactic gaps
226 (Table 2). Each vowel-liquid pairing was elicited adjacent to a labial onset or coda consonant, to minimize
227 95
228 coarticulatory effects on the target nucleus. In some cases, it is not clear exactly which segment best
229 represents the vowel before a rhotic-final coda, and some contrasts may be partially or fully neutralized for
230
231

237
238
239
240
241
242 some speakers. In particular, /eɪ/ may be monophthongal [e] in pre-lateral and pre-rhotic contexts, and
243 /oʊ/ may be realized as [oʊ], [o], or [ɔ], depending on speaker and context. Bearing all these factors
244 in mind, the experimental materials were designed to elicit all potentially contrastive liquid-final rimes of
245 General American English.
246
247

248 In addition to these vowel-liquid and liquid-vowel sequences, all vowels were elicited in monosyllabic
249 words with labial onsets and codas (Table 2, last column) to capture intrinsic vowel targets in lexical items
250 with minimal lingual coarticulatory influence from surrounding consonants. Laterals (*‘lime’, ‘pile’, ‘Lao’,*
251 *‘fowl’, ‘larm’, ‘pearl’*) and rhotics (*‘rhyme’, ‘fire’, ‘Rao’, ‘bour’, ‘fur’*) were also produced adjacent to the
252 diphthongs /aɪ/ (*‘vibe’*) and /aʊ/ (*‘pow’*) and the rhoticized vowel /ɜ˞/ (*‘verb’*), to capture the full range of
253 phonotactic environments in which both liquids may appear in General American English. These data were
254 examined qualitatively, but were not included in the quantitative analyses because they were not directly
255 comparable with liquids produced adjacent to the other vowels: nuclear targets were temporally complex,
256 produced inconsistently across speakers, and/or indistinguishable from rhotic-initial codas.
257
258
259
260

261
262 Table 2: **Experimental Materials: Elicitation Items**

| CONTEXT | ONSET | | CODA | | VOWEL |
|---------|-------|-------------------|------|-------------------|-------|
| | #l | #ɹ | l# | ɹ# | |
| /i/ | leap | reap | peel | | beep |
| /ɪ/ | lip | rip | pill | beer | bib |
| /eɪ/ | lame | rave | bail | | babe |
| /ɛ/ | Lev | rep | bell | bare | pep |
| /æ/ | lap | rap | pal | | bam |
| /ʌ/ | love | rum | mull | | pub |
| /ɑ/ | lob | rob | ball | bar | bob |
| /oʊ/ | lobe | robe | pole | bore | foam |
| /u/ | loop | ¹ rube | pool | ² boor | boom |
| /ʊ/ | loof | | pull | | boof |

281
282 Five repetitions were elicited for each word with a liquid target, and two repetitions of each vowel target
283 item. Words were presented in pseudo-randomized order, in blocks containing up to 13 items. Nonce words
284

285 ¹Although [ʊ] is attested after [ɹ] in *‘rook’* [ɹʊk] in General American English, the [u/ʊ] contrast is neutralized after [ɹ]
286 before a labial coda, with some variability in realization of the vowel. For instance, some speakers pronounce *‘room’* as [ɹʊm]
287 and others as [ɹʊm] (Wells, 2008).

288 ²Three of our subjects reported a full or partial merger of back round vowels to [ɔ] before a coda rhotic. Nevertheless, they
289 attempted to produce *‘boor’* with a high back vowel.

296
297
298
299
300
301 whose vocalic pronunciation was not obvious from their spelling were reviewed in advance with the subjects
302 for their intended pronunciation, and were elicited along with a rhyming word as a reminder, (e.g. ‘woof’
303 for ‘boof’). In addition to the core experimental corpus, four short read passages and some spontaneous
304 115 for ‘boof’). In addition to the core experimental corpus, four short read passages and some spontaneous
305 speech was elicited from each participant, in recording sessions lasting up to 70 minutes.
306

307 2.3. Image and Audio Acquisition

308
309 MRI data were acquired at Los Angeles County Hospital on a Signa Excite HD 1.5T scanner, using a
310 custom upper airway receiver coil array. Each subject’s upper airway was imaged while they lay supine
311 in the MRI scanner with their head immobilized. Elicitation items were presented one word at a time, in
312 120 in the MRI scanner with their head immobilized. Elicitation items were presented one word at a time, in
313 large text on a back-projection screen which subjects could read from within the scanner bore. Participants
314 adopted similar oral resting postures between utterances: lips closed (W2, W3, M1) or slightly open (W1),
315 tongue tip resting on (W2, W3, M1) or just below (W1) the alveolar ridge, and tongue body resting on
316 (W2) or just below (W1, W3, M1) the hard palate. Rest postures were consistently maintained by each
317 participant throughout the experiment, suggesting that there were no major effects of articulatory setting
318 125 participant throughout the experiment, suggesting that there were no major effects of articulatory setting
319 on patterns of production within or across subjects.
320
321

322 A gradient echo pulse sequence (13 interleaved spiral readout; max. gradient = 4.0 G/cm; max. slew
323 rate = 15.0 G/cm/ms; TR = 6.164 ms) was used to acquire a 5 mm midsagittal slice with image resolution
324 68 × 68 pixels over a 200 × 200 mm field of view. Image data were reconstructed as 23.2 frames per second
325 video sequences (Bresch et al., 2008). Audio was simultaneously recorded at a sampling frequency of 20kHz
326 130 video sequences (Bresch et al., 2008). Audio was simultaneously recorded at a sampling frequency of 20kHz
327 inside the MRI scanner while subjects were imaged, using a custom fiber-optic microphone noise-canceling
328 system (Bresch et al., 2006).
329
330

331 2.4. Articulatory Analysis

332 MRI data and companion audio were loaded into a custom graphical user interface for inspection and
333 analysis (Proctor et al., 2010; Narayanan et al., 2014). For each token in the corpus, the interval of image
334 135 analysis (Proctor et al., 2010; Narayanan et al., 2014). For each token in the corpus, the interval of image
335 frames containing the utterance was first located using acoustic landmarks. Frame numbers corresponding
336 to articulatory targets were then identified in the MRI video using the following criteria:
337

- 338 • *lateral coronal target*: first frame after completion of tongue tip (TT) constriction, or maximum
339 advancement of TT within acoustic interval of utterance when no coronal constriction is achieved
340
- 341 • *lateral dorsal target*: max. tongue body (TB) retraction during lateral production interval
342 140 • *lateral dorsal target*: max. tongue body (TB) retraction during lateral production interval
343
- 344 • *rhotic labial target*: max. labial (LAB) compression/protrusion during rhotic production interval
345
- 346 • *rhotic dorsal target*: max. TB retraction/lowering during rhotic production interval
347
348
349

- *rhotic coronal target*: closest approximation of front of tongue to palate during rhotic production interval
- *vowel target posture*: center frame of most stable interval associated with primary vocalic goal (corresponding to monophthongal vowel target after any on-glide, or first target of diphthongs)

Landmarks were identified by manual inspection of the speech interval of interest, reviewing the video sequences frame-by-frame, forward and reverse, until the video frame which optimally satisfied the selection criteria was located. Coronal and labial landmarks were identified as the frame in which pixel brightness was maximized in the region of the target constriction, since mean pixel intensity is correlated with the amount of soft tissue in a region in rtMRI (Proctor et al., 2011). Landmark analysis was performed with reference to the entire tip and body of the tongue – making use of the global view of lingual configuration provided by rtMRI – rather than tracking specific flesh-points on these articulators, as in EMA analysis.

Tissue Boundary Location. Reference vocal tract outlines were located for each speaker in the palate and pharynx using mean image sets, and superimposed on each image frame to define passive tract boundaries. Midsagittal tongue and lip outlines were then located in each MRI frame in the sequences of interest (Fig. 1), using a tissue tracking algorithm operating over intensity profiles constrained by a semi-polar analysis grid (details in Proctor et al., 2010).

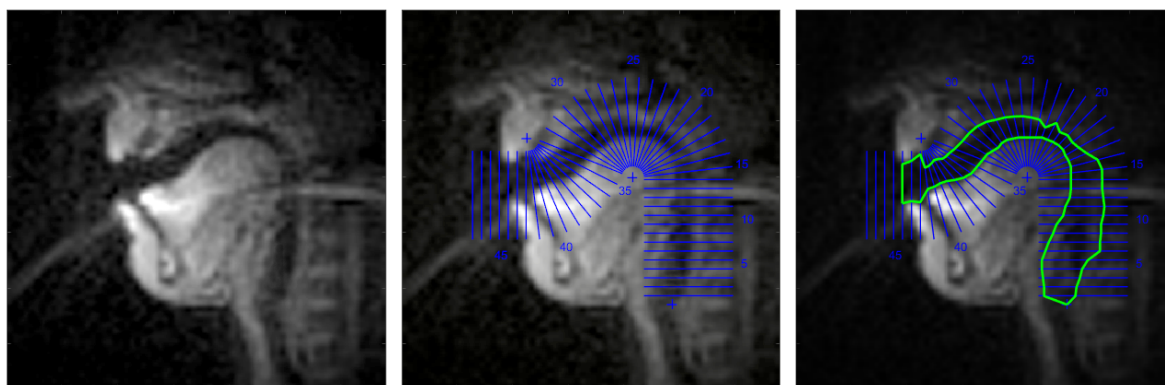
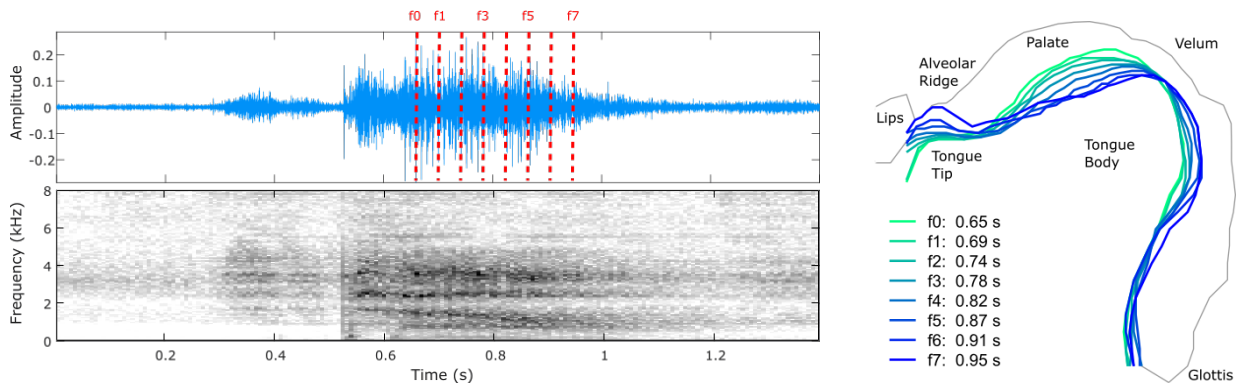


Figure 1: **Midsagittal tissue boundary segmentation in rtMRI data.** Left: Image frame captured at articulatory target of low front vowel after onset lateral (Subject M1: ‘lap’). Centre: Semi-polar vocal tract analysis grid (blue radial lines) superimposed on image; Right: tissue boundaries (green outline) located from pixel intensity thresholds. Arc-shaped artifact passing through lower lip, tongue body and pharynx caused by co-planar cardiac activity.

Tracking Change in Midsagittal Articulation. Sequences of tongue edges were extracted from the temporal intervals demarcated by the landmarks defined in §2.4. These image sequences show change in lingual posture from coronal consonant targets to vowel target for onsets, and from vowel to coronal consonant

414
 415
 416
 417
 418
 419 targets for coda liquids (Fig. 2). At each articulatory landmark of interest, tongue edges were extracted
 420 from each token so that mean tongue postures could be calculated and compared. Tongue postures were
 421 extracted from the second, third and fourth repetitions of each word. The first repetition, produced while
 422 the participants adjusted to the task of reading prompted speech in a noisy MRI scanner, was excluded from
 423 the analysis in case these utterances were atypical or erroneous; the fifth repetition was used in cases where
 424 one of the previous tokens was mispronounced, so that three tokens were analyzed for each vowel-liquid and
 425 liquid-vowel sequence.
 426
 427
 428



430
 431
 432
 433
 434
 435
 436
 437
 438
 439
 440
 441 **Figure 2: Tracking change in midsagittal lingual posture.** Left: speech waveform (top) and spectrogram
 442 (bottom) of lateral-final utterance (Subject M1: 'pal'). Right: tongue edges captured at 43 ms intervals, from nuclear
 443 vowel target (green) to coda posture at lateral coronal target (blue). Broken (red) lines superimposed on waveform
 444 show points in time and image frame numbers from which each tongue edge is captured in articulatory sequence.
 445 Spectrogram shows broadband background noise characteristic of in-scanner speech recordings.
 446
 447

448
 449 *Mean Articulatory Targets.* Characteristic midsagittal lingual postures associated with segments of interest
 450 were derived by calculating mean tongue positions at equivalent points in time across multiple tokens.
 451 Average target tongue shapes of rhotics and laterals produced by each speaker were generated by calculating
 452 the Euclidean mean point on each analysis gridline, from the set of all exemplars of each consonant. Mean
 453 lingual outlines were calculated from 33 tokens of each speaker's onset rhotic (3 repetitions \times 11 vowel
 454 contexts), 39 tokens of each onset lateral (3 \times 13 vowel contexts), 24 tokens of each speaker's coda rhotic
 455 (3 \times 8 vowel contexts), and 39 tokens of each coda lateral (3 \times 13 vowel contexts).
 456
 457

458
 459 *Coarticulatory Influence.* The coarticulatory influence of liquid consonants on tautosyllabic vowels was
 460 estimated by comparing mean tongue posture at vowel target in liquid-initial and liquid-final words³ with the
 461 shape of the tongue captured during separate production of the same vowel in an inter-labial context (Table
 462 2, rightmost column). The Euclidean distance between the two mean tongue edges was calculated along
 463
 464

465
 466 ³What the intrinsic vowel target is before a rhotic deserves consideration. We return to this issue in Section 3.6.
 467

473
474
475
476
477
478
479
480
481
482
483
484
485
486
487
488
489
490
491
492
493
494
495
496
497
498
499
500
501
502
503
504
505
506
507
508
509
510
511
512
513
514
515
516
517
518
519
520
521
522
523
524
525
526
527
528
529
530
531

each analysis gridline over the length of the tongue, from the sublingual cavity to the tongue root (Fig. 3). Total lingual displacement from intrinsic vocalic posture was calculated as the sum of all distances (mm) between the two mean tongue postures: the higher the sum of distances, the greater the total displacement of the lingual shape in a vowel, attributable to the coarticulatory influence, or ‘aggressiveness’ (Farnetani, 1990; Fowler & Saltzman, 1993; Recasens & Espinosa, 2009), of the adjacent consonant.

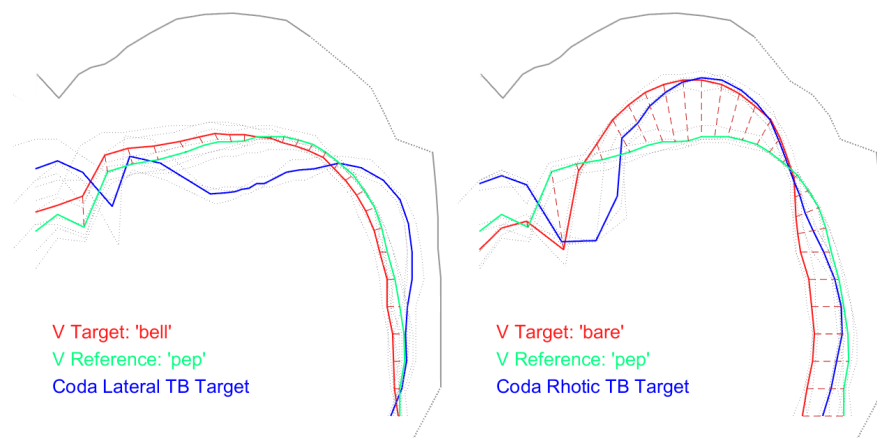


Figure 3: **Quantifying Consonant-Vowel Coarticulation.** Green tongue outline: intrinsic posture of vowel [ɛ] in inter-labial context (‘*pep*’), where coarticulatory influences are minimal. Solid red lines: mean lingual postures of same vowel produced adjacent to liquid consonants. Blue lines: mean tongue posture at dorsal target of tautosyllabic liquid. Lingual displacement due to coarticulatory influence of consonant is calculated as total Euclidean distance between vowel postures along all analysis gridlines intersecting the tongue between sublingual cavity and tongue root (broken red connecting lines). Left: [ɛ] before coda lateral (‘*bell*’); Right: [ɛ] before coda rhotic (‘*bare*’). (All comparisons: Speaker W1).

Coarticulatory Resistance. Coarticulatory resistance (Bladon & Al Bamerni, 1976; Recasens, 1984) of liquid consonants was estimated by examining variability in tongue shaping across a set of liquid tokens produced in different vocalic contexts. Consonants produced before and after the common set of vowels /ɪ-ɛ-ɑ-ou-ʊ/ were captured at the dorsal target frame, and mean tongue postures were calculated from all repetitions of the same liquid in the same syllable context. The Euclidean distance between each tongue edge and the mean posture was calculated at each point along the subset of gridlines extending from the midsagittal cavity to the tongue root-epiglottal junction. Variance of displacement from mean tongue posture was also calculated at each gridline for each set of tongue edges representing the same liquid allophone (Fig. 4). Mean total displacement and mean total variance (averages of group means and variances calculated at each gridline) were calculated to estimate coarticulatory resistance across the common set of context vowels.

532
533
534
535
536
537
538
539
540
541
542
543
544
545
546
547
548
549
550
551
552
553
554
555
556
557
558
559
560
561
562
563
564
565
566
567
568
569
570
571
572
573
574
575
576
577
578
579
580
581
582
583
584
585
586
587
588
589
590

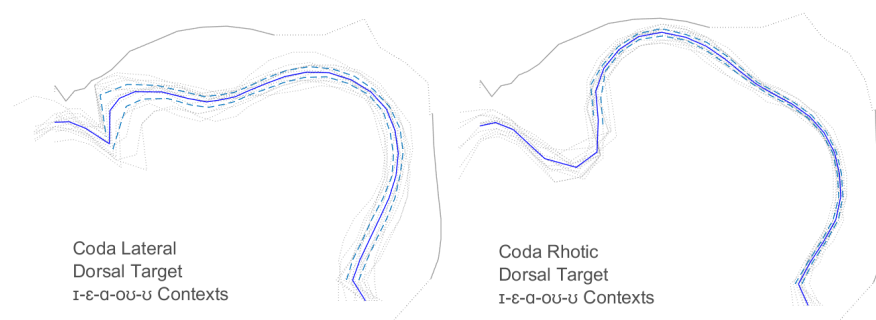


Figure 4: **Quantifying Coarticulatory Resistance.** Variance in displacement from mean posture of coda liquids following vowels /I-ε-ɑ-ou-u/. Left: coda lateral; Right: coda rhotic (Speaker W2). Light grey lines: tongue posture at dorsal target in each liquid token. Blue solid lines: mean tongue posture across all tokens. Blue dashed lines delimit two standard deviations of displacement from mean tongue posture: greater separation indicates greater variance in tongue shape at consonantal target due to coarticulatory effects of adjacent vowel.

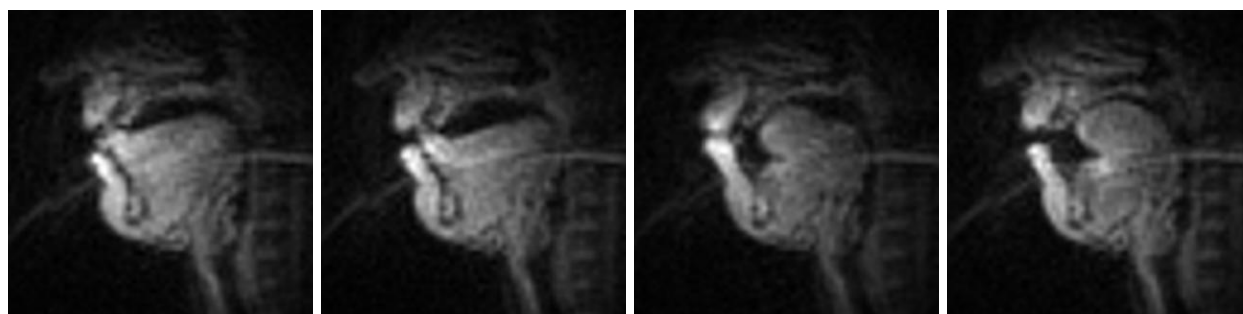
195 2.5. Statistical Analysis

Because of the small number of participants, and consistent with the goals of the study, details of individual liquid production are reported, along with statistical analyses of the major patterns of production identified across all speakers. Statistical analysis was conducted in R version 3.5.1 (R Core Team, 2018). Linear mixed effects models were fitted with the *lme4* package (Bates et al., 2015) using restricted maximum likelihood (REML). The optimal model for each analysis was determined to be the one with the lowest Akaike Information Criterion (AIC) among candidate models refitted using maximum likelihood (ML) to maximize
200 goodness-of-fit. Individual speaker differences were modelled using random intercepts for SUBJECT unless models with by-speaker random slopes for fixed effects provided a significantly better fit (χ^2 tests, $p < 0.05$). Simpler models were also used when fitted vs. residual plots of extended models revealed large deviations
205 from linearity or when residual quantile–quantile plots revealed large deviations from normality, and when models failed to converge due to data sparsity or imbalance. *t*-statistics, *F*-statistics, and corresponding *p*-values were calculated with the *lmerTest* package (Kuznetsova et al., 2017) using Satterthwaite’s method for denominator degrees of freedom.

Standardized effect sizes and power analyses are also reported to facilitate interpretation of the results
210 with respect to the scope of the study (Kirby & Sonderegger, 2018). Standardized effect sizes (*d*) were calculated with variance components (Brysbaert & Stevens, 2018), using the method for fully-crossed designs in mixed effects models described in Westfall et al. (2014). Power estimates were conducted with Monte Carlo simulations, using the *simr* package (Green & MacLeod, 2016). Power calculations were made over 1,000 simulations at a significance level of $\alpha = 0.05$, using Type-II tests with Satterthwaite denominator
215 degrees of freedom.

591
592
593
594
595
596 **3. Results**
597

598 We first describe the articulatory characteristics of each liquid as revealed by rtMRI: the gestures as-
599 sociated with each consonant at each syllable margin, and the ways that they differ between speakers and
600 allophones. Gestural characterization of each liquid establishes a set of common landmarks for reference in
601 the analysis of coarticulation, and provides a validation of these data in broad strokes against what is known
602 220 from previous studies about the articulation of liquids. To illustrate the tongue postures characteristic of
603 each liquid at each syllable margin, laterals and rhotics produced in a low vowel context by Speaker M1 are
604 juxtaposed in Fig. 5.
605
606
607



618 **Figure 5: Illustrative Liquid Postures: Low Vowel Context, Subject M1.** Left-to-right: Onset lateral ‘lob’, coda lateral
619 ‘ball’, onset rhotic ‘rob’, coda rhotic ‘bar’. Tongue captured at coronal target of each liquid.
620

621
622
623 *3.1. Articulatory Characterization of Lateral Allophones*

624 225 Mean tongue postures for word-initial laterals are contrasted with mean coda lateral postures in Fig. 6.
625 Onset laterals were produced with an apical coronal closure against the back of the upper incisors (Fig. 5, left
626 panel), accompanied by retraction of the tongue body towards a uvular (W2, W3, M1) or pharyngeal (W1)
627 target (Fig. 6). Coda laterals were produced with the same two gestures; however, complete constriction
628 of the tongue-tip against the teeth or alveolar ridge was achieved much less consistently than in initial
629 allophones. All coda laterals of W3 and M1 concluded with full TT closure, but none of the 30 word-final
630 laterals were produced by W1 with full tongue-tip closure. In 13% of W2’s final laterals coronal closure was
631 230 not achieved before the acoustic end of the utterance. In the most vocalized coda lateral realizations (those
632 with the greatest degree of lenition of the anterior gesture in the midsagittal plane: Fig. 6, left panel), the
633 tongue tip approached no closer to the alveo-dental target than 10 mm (W1 ‘pal’) and 8 mm (W1 ‘pool’).
634
635
636
637

638 235 Individual speakers differ in the positioning of the tongue body in lateral production: M1, W2 and W3
639 retract the rear of the tongue towards the uvula, consistent with previous descriptions of American English
640 /l/ (Giles & Moll, 1975; Bladon & Al Bamerni, 1976), while the posterior gesture of W1’s lateral is lower
641 and post-uvular, and better characterized as having a mid-pharyngeal target, even in onset position (Fig. 6,
642
643
644

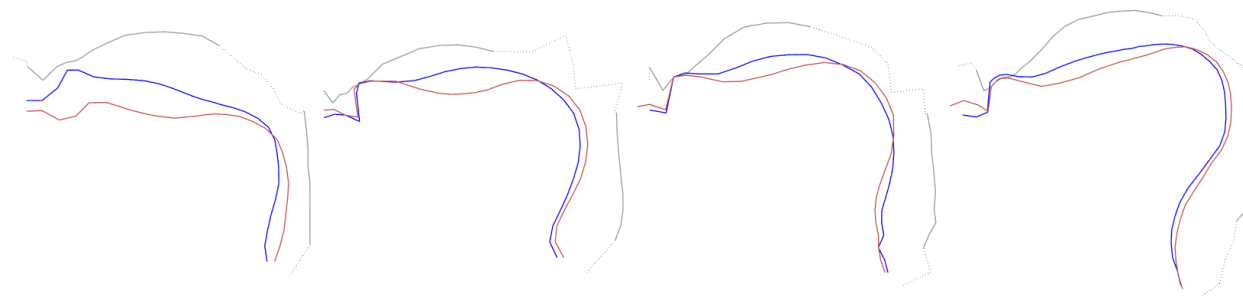


Figure 6: **Mean Lateral Articulatory Postures: Onsets vs. Codas, all Vowel Contexts.** Blue lines: mean midsagittal tongue shape at onset coronal target (all lateral-initial tokens); Red lines: mean midsagittal tongue shape at coda coronal target (all lateral-final tokens); Left-to-right: Subjects W1, W2, W3, M1. Grey lines depict palatal and pharyngeal outlines. Broken grey lines show indicative posture of (variably articulated) soft palate and lower pharynx.

left panel). The minimal constriction between the back of the tongue and the rear pharyngeal wall/uvula was located 65 mm above the glottis for M1, and 27 mm above the glottis in mean coda posture for W1.

The rearmost part of the tongue body was, on average, more retracted in word-final laterals produced by all speakers (Fig. 6). The grand mean difference in TB retraction between onset and coda laterals (all speakers, all tokens) was -2 mm. Mean minimum pharyngeal aperture was 2 mm more constricted in coda laterals, compared to onsets. For all speakers, the front of the dorsum is lower in coda [l], compared to the onset lateral: the height difference – measured at the point of greatest difference between mean lateral postures posterior to the tongue blade – varied from 6 mm (M1) to 10 mm (W1); the mean greatest difference in dorsal tongue height between onset and coda laterals across all speakers was 7 mm. W1 also showed the greatest difference in coronal articulation between positional allophones: her coda laterals were produced without complete tongue tip closure in the midsagittal plane, and her mean coda lateral posture is highly vocalized, displaying a large aperture (14 mm) between the closest point of excursion of the tongue tip to the alveolar ridge (Fig. 6, left panel).

3.2. Articulatory Characterization of Rhotic Allophones

Mean midsagittal tongue postures for rhotic approximants produced in syllable onset position are compared with mean postures for coda rhotics⁴ in Fig. 7. Three gestures could be identified in word-initial rhotics produced by all speakers: labial approximation, coronal approximation towards the palate, and tongue root retraction/lowering (e.g. Fig. 5, 3rd panel). Labial approximation – sometimes accompanied by lip protrusion – was clearly observed in all 108 onset rhotics analyzed (27 tokens \times 4 speakers), as was the onset rhotic coronal gesture. Retraction of the tongue body towards the lower rear pharyngeal wall

⁴Some details of the geometry of sublingual cavities may appear simplified in figures illustrating mean tongue outlines, as a result of averaging of air-tissue boundaries across analysis gridlines spaced up to 5 mm apart.

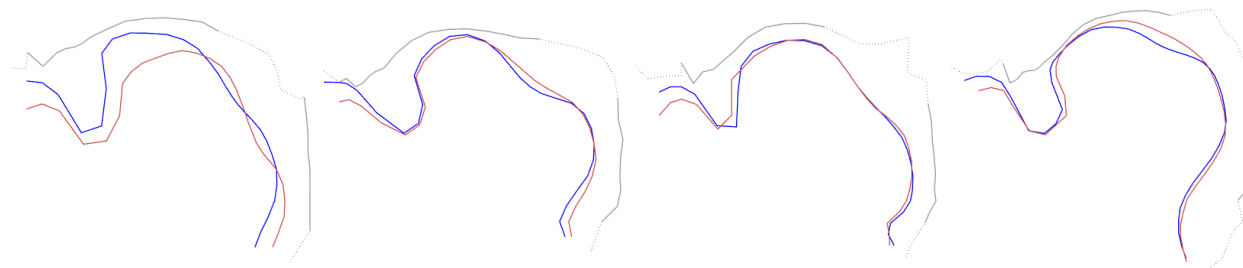


Figure 7: **Mean Rhotic Articulatory Postures: Onsets vs. Codas, all Vowel Contexts.** Blue lines: mean midsagittal tongue shape at onset coronal target (all rhotic-initial tokens); Red lines: mean midsagittal tongue shape at coda coronal target (all rhotic-final tokens); Left-to-right: Subjects W1, W2, W3, M1. Grey lines depict palatal and pharyngeal outlines.

was observed in all word-initial rhotics, accompanied by a tongue root lowering gesture at the base of the epiglottis, towards the glottis. Although the dorsal retraction associated with rhotic production was not always distinguishable from the tautosyllabic vowel gesture, some lowering of the tongue root was identifiable in onset rhotics produced before all vowels.

Coda rhotics were characterized by a dorsal gesture produced before, or at the same time as, approximation of the front of the tongue towards the palate (Figs. 9, 11, 13, 15, bottom rows). There was no evidence of a labial gesture in coda rhotics produced by speakers W1, W3, and M1 (Fig. 5, right panel); even in words containing a rounded vowel (*'bore'*, *'boor'*, *'bour'*), the lips invariably moved apart in the transition from the nucleus to the rhotic coda. Some lip protrusion accompanied the coda rhotic in two utterances of *'beer'* by W2, but as with the other speakers, no labial approximation was observed in word-final rhotics produced by W2 after any vowel.

Individual speakers' rhotics vary in how bunched the tongue is, and in the degree and location of the oral constrictions (Fig. 7). Coronal constrictions range in anteriority, with part of the tongue approaching a post-alveolar target in the most advanced realizations (M1), but all speakers' rhotics are articulated with a large mass of the front part of the tongue approximating the hard palate. The minimum mean aperture of the coronal constriction ranges from 1 mm (M1 onset and coda) to 14 mm (W1 coda). The most constricted part of the posterior oral cavity is located low in the pharynx for Speaker W1 (13 mm above the glottis in mean coda posture), in the upper pharyngeal region for M1 (58 mm above the glottis in mean onset posture), and at mid-pharyngeal positions for W2 and W3 (mean 30 mm above glottis).

Despite these individual differences, the word-initial rhotics produced by all four speakers are characterized by five shared midsagittal articulatory properties: (i) bilabial approximation; (ii) a prominent sublingual cavity; (iii) approximation of a broad part of the front of the tongue towards the post-alveolar/palatal region; (iv) a pharyngeal constriction; and (v) a region of concave curvature in the middle of the tongue (a mid-dorsal saddle). Midsagittal tongue shapes of coda rhotics closely resemble those produced in syllable on-

768 set position by the same speakers. The most pronounced difference between the two mean postures is the ab-
 769 sence of labialization in coda /ɹ/. Linear mixed models with random intercepts for subject were constructed
 770 to test the effects of syllable position (onset/coda) on labial posture on rhotics (measured at the coronal
 771 target frame). Labial aperture is more constricted in onsets ($\beta = -9.2$ mm, $t(163) = -18.8$, $p < 0.001$; $d = -$
 772 1.97, POWER = 100%), and lips are more protruded in onset rhotics ($\beta = 5.7$ mm, $t(163) = 11.72$, $p < 0.001$;
 773 $d = 1.20$, POWER = 100%), compared to coda allophones. (Details of statistical models in Appendix A).
 774

782 3.3. Gestural Coordination in Liquids

783 Mean inter-gestural timing relationships for laterals produced by each speaker are summarized in Table
 784 3; mean gestural lags for rhotics are given in Table 4. For each speaker, mean time of achievement of tongue
 785 tip and tongue body gestures are calculated relative to the articulatory target of the nuclear vowel ($t = 0$)
 786 in each token. For onset rhotics, mean time of maximum labial approximation is also reported. Because
 787 the rtMRI data are acquired at 23.2 f.p.s., timing differences smaller than 43 ms cannot be resolved without
 788 interpolation, and mean lag calculations are clustered around integral multiples of this minimum timeslice
 789 (86 ms = 2 frames; 129 ms = 3 frames; etc.). Despite these limitations, these data reveal clear intergestural
 790 timing patterns and ordering relationships associated with the allophones of each liquid.
 791

792 Table 3: **Mean Inter-gestural Timing for Lateral Allophones.**

793 TT: tongue-tip closure; TB: maximum retraction of tongue body. Mean (s.d.)
 794 timings from 30 utterances: three repetitions of each liquid in ten different
 795 vocalic contexts (Table 2). All times (ms) calculated w.r.t. frame in which
 796 tongue body achieves vowel target (V).
 797

| | ONSET LATERAL | | | CODA LATERAL | | |
|--------------|---------------|-----------|---|--------------|----------|----------|
| | TT | TB | V | V | TB | TT |
| W1 | -265 (57) | -181 (60) | 0 | 0 | 253 (72) | 506 (87) |
| W2 | -292 (43) | -198 (39) | 0 | 0 | 165 (67) | 288 (44) |
| W3 | -278 (45) | -187 (43) | 0 | 0 | 144 (77) | 282 (53) |
| M1 | -262 (53) | -183 (48) | 0 | 0 | 219 (85) | 298 (58) |
| Mean: | -274 (50) | -187 (47) | 0 | 0 | 195 (75) | 343 (61) |

803 In onset position, lateral production invariably commences with tongue-tip closure, achieved approximately
 804 90 ms before the tongue body reaches its point of maximum retraction. The post-lateral vowel reaches
 805 its articulatory target approximately 190 ms after the dorsal gesture. Coda laterals are realized with the
 806 reverse temporal sequencing of gestures: maximum dorsal retraction is achieved approximately 200 ms after
 807

the vowel reaches its gestural target, followed 150 ms later (grand mean) by coronal closure or maximum tongue tip advancement.

Table 4: **Mean Inter-gestural Timing for Rhotic Allophones.** LAB: maximum labial approximation; TT: tongue-tip closure; TB: tongue body/root gestural target. Mean (s.d.) onset timings from 27 utterances: three repetitions of each rhotic in nine different vowel contexts. Mean coda timings from 15 utterances: three repetitions of each rhotic after five different vowels (Table 2). All times (ms) calculated w.r.t. frame in which tongue body achieves vowel target (V).

| | ONSET RHOTIC | | | | CODA RHOTIC | | |
|--------------|--------------|-----------|-----------|---|-------------|----------|----------|
| | LAB | TT | TB | V | V | TB | TT |
| W1 | -249 (55) | -219 (59) | -219 (59) | 0 | 0 | 244 (53) | 351 (46) |
| W2 | -248 (47) | -219 (46) | -219 (46) | 0 | 0 | 193 (32) | 285 (43) |
| W3 | -221 (55) | -205 (52) | -205 (49) | 0 | 0 | 193 (32) | 259 (36) |
| M1 | -198 (42) | -187 (41) | -187 (41) | 0 | 0 | 253 (63) | 302 (49) |
| Mean: | -229 (50) | -207 (49) | -207 (49) | 0 | 0 | 221 (45) | 299 (43) |

Onset rhotic production is initiated with labial approximation, which reaches its target – a narrow labial constriction typically accompanied by some protrusion – immediately prior to, or at the same time that the two lingual gestures reach their targets. On average, the labial gesture precedes the lingual gestural targets by 20 ms (grand mean). In all onset rhotics, tongue tip and tongue body/root gestures reached their respective targets within the same frame, approximately 200 ms before the vowel gesture. Word-final rhotics are not characterized by the same synchrony of lingual gestures. In three utterances of ‘beer’ by M1, the dorsal and coronal gestures reach their targets in the same frame, but in all other coda rhotics, the posterior gesture precedes the anterior gesture. On average, the TB target is achieved 220 ms after the vocalic target, followed 80 ms later by the coronal gesture.

Linear mixed models with random intercepts for subject were constructed to test the effects of consonant type on the relative timing of lingual gestures at each syllable margin. All timings are expressed with respect to the nucleus, so that gestures achieved before the vowel target (V) have a negative lag, and coda gestures have a positive lag. Consonant type was treatment coded (LATERAL = 0; RHOTIC = 1) so that model intercepts correspond to lag estimates for laterals, and beta coefficients represent the effect of rhotics on lag. In onsets, TT–V lag is shorter for rhotics ($\beta = 66$ ms, $t(223) = 9.98$, $p < 0.001$; $d = 1.29$, POWER = 100%), and TB–V lag is longer for rhotics ($\beta = -20$ ms, $t(223) = -3.17$, $p = 0.0018$; $d = -0.41$, POWER = 89.6%) compared to laterals. In codas, V–TT lag is shorter for rhotics ($\beta = -44$ ms, $t(175) = -4.34$, $p < 0.001$; $d = -0.42$, POWER = 99.2%), V–TB is longer for rhotics ($\beta = 26$ ms, $t(175) = 2.40$, $p = 0.018$; $d = 0.32$, POWER = 65.1%),

886
887
888
889
890
891 and TB–TT is shorter for rhotics ($\beta = -70$ ms, $t(175) = -7.82$, $p < 0.001$; $d = 0.88$, POWER = 100%) compared
892 to laterals. Details of all statistical analyses are provided in Appendix B. Residual analyses suggest that
893 these models are robust (quantile-quantile and fitted vs. residual plots showed residuals to be broadly
894 normally distributed and homoscedastic), and power analyses indicate that the data are able to robustly
895 discriminate all timing differences except the V–TB lag in codas. Nevertheless, these results should be
896 interpreted with caution, bearing in mind that the temporal resolution of the data is 43 ms.

900 3.4. Patterns of Onset and Coda Liquid Coarticulation

901
902 Having identified each speaker’s characteristic tongue shape at rhotic and lateral targets, we tracked
903 the change in tongue shape over time as liquid consonants were coproduced with different vowels. Image
904 sequences showing the evolution of lingual configuration between vocalic and liquid articulatory landmarks
905 were superimposed using the method illustrated in Fig. 2, to examine specific patterns of coarticulation for
906 rhotics and laterals, and to see how these patterns vary between onsets and codas.

909 *Liquid Articulation in Front Vowel Contexts.* Lateral approximants produced before and after the high front
910 vowel /ɪ/ are compared in Fig. 8. The coarticulatory influence of the following vowel on word-initial laterals
911 can be seen in the blue (consonantal) frames (Fig. 8, top row), where the front of the dorsum (mid region
912 of the tongue beneath the palate) overlaps more closely with the vowel posture (green frames), compared
913 to the lateral-final sequences (Fig. 8, bottom row). The saddle between the front and back of the tongue is
914 more convex for all speakers’ [l] in ‘pill’, compared to ‘lip’.

917 For all four speakers, rhotics produced before /ɪ/ show considerable dorsal overlap between consonantal
918 and vocalic postures in the pharyngeal region (Fig. 9, top row). Coda rhotics produced after the same vowel
919 (Fig. 9, bottom row) involve greater displacement of the back of the tongue towards the rear pharyngeal
920 wall in the transition from vowel to coda in ‘beer’. The most notable asymmetry for rhotics produced in
921 this vowel context is the greater overlap of vocalic and consonantal tongue posture in the coronal region for
922 word-final rhotics compared to their word-initial allophones, which are characterized by greater displacement
923 of the front part of the tongue in the transition into the following vowel in ‘rip’.

927 Laterals and rhotics produced before and after a mid front vowel are compared in Figs. 10 and 11. The
928 same patterns and asymmetries observed in the high front vowel context are also evident here: onset laterals
929 (‘Lev’) show less mid-dorsal displacement from the posture of the tautosyllabic vowel compared to coda
930 laterals (‘bell’), and little displacement can be seen between consonantal and vocalic postures in the lower
931 pharyngeal region in either syllable context. As in the /ɪ/ context, coda rhotics produced after /ɛ/ (‘bare’)
932 show more tongue root retraction and greater coronal overlap between vocalic and consonantal postures
933 than in onset position (‘rep’), where greater anterior lingual displacement is observed compared to ‘bare’.
934 Similar patterns of articulation to those illustrated in Figs. 8–11 are also observed for liquids produced in
935 /i/ (‘leap’, ‘peel’, ‘reap’), /eɪ/ (‘lame’, ‘bail’, ‘rave’), and /æ/ (‘lap’, ‘pal’, ‘rap’) contexts.

945
946
947
948
949
950
951
952
953
954
955
956
957
958
959
960
961
962
963
964
965
966
967
968
969
970
971
972
973
974
975
976
977
978
979
980
981
982
983
984
985
986
987
988
989
990
991
992
993
994
995
996
997
998
999
1000
1001
1002
1003

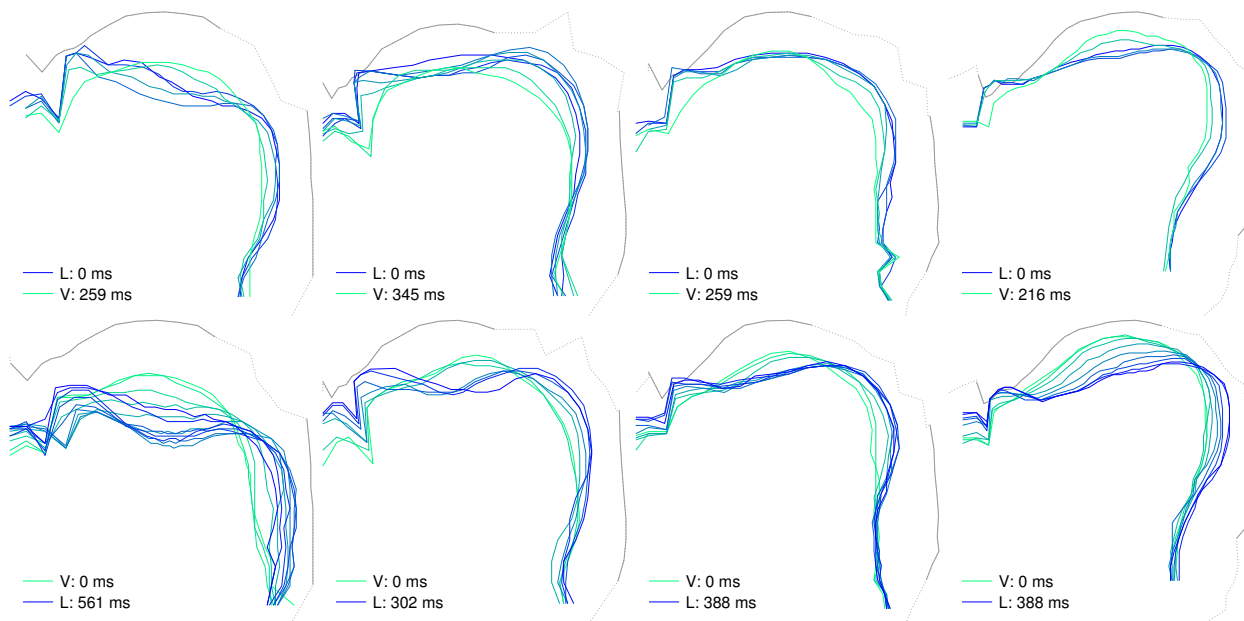


Figure 8: **Lateral Production in High Front Vowel Context.** Top row: onset (*'lip'*); Bottom row: coda (*'pill'*); Left-to-right: Speakers W1, W2, W3, M1; Blue lines: tongue posture at lateral coronal target; Green lines: vowel target posture. Intermediate colors: tongue postures captured at 43 ms intervals in the transition between lateral and vowel.

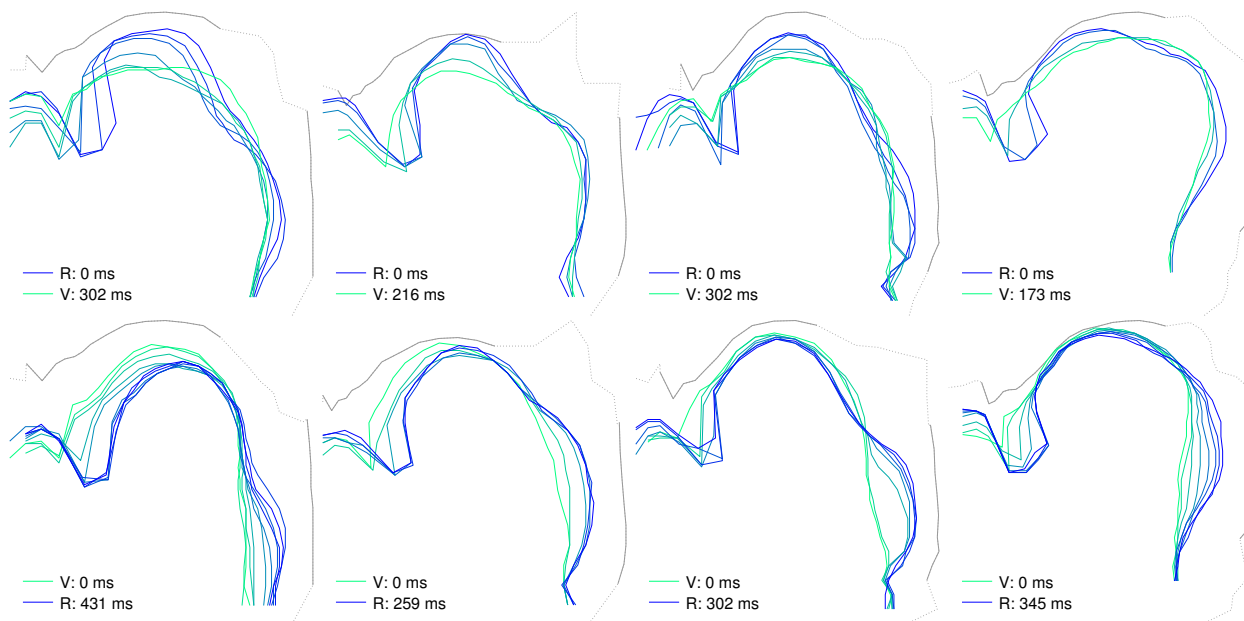


Figure 9: **Rhotic Production in High Front Vowel Context.** Top row: onset (*'rip'*); Bottom row: coda (*'beer'*); Left-to-right: W1, W2, W3, M1; Blue lines: tongue posture at rhotic coronal target; Green lines: vowel target posture. Intermediate colors: tongue postures captured at 43 ms intervals in the transition between rhotic and vowel.

1004
 1005
 1006
 1007
 1008
 1009
 1010
 1011
 1012
 1013
 1014
 1015
 1016
 1017
 1018
 1019
 1020
 1021
 1022
 1023
 1024
 1025
 1026
 1027
 1028
 1029
 1030
 1031
 1032
 1033
 1034
 1035
 1036
 1037
 1038
 1039
 1040
 1041
 1042
 1043
 1044
 1045
 1046
 1047
 1048
 1049
 1050
 1051
 1052
 1053
 1054
 1055
 1056
 1057
 1058
 1059
 1060
 1061
 1062

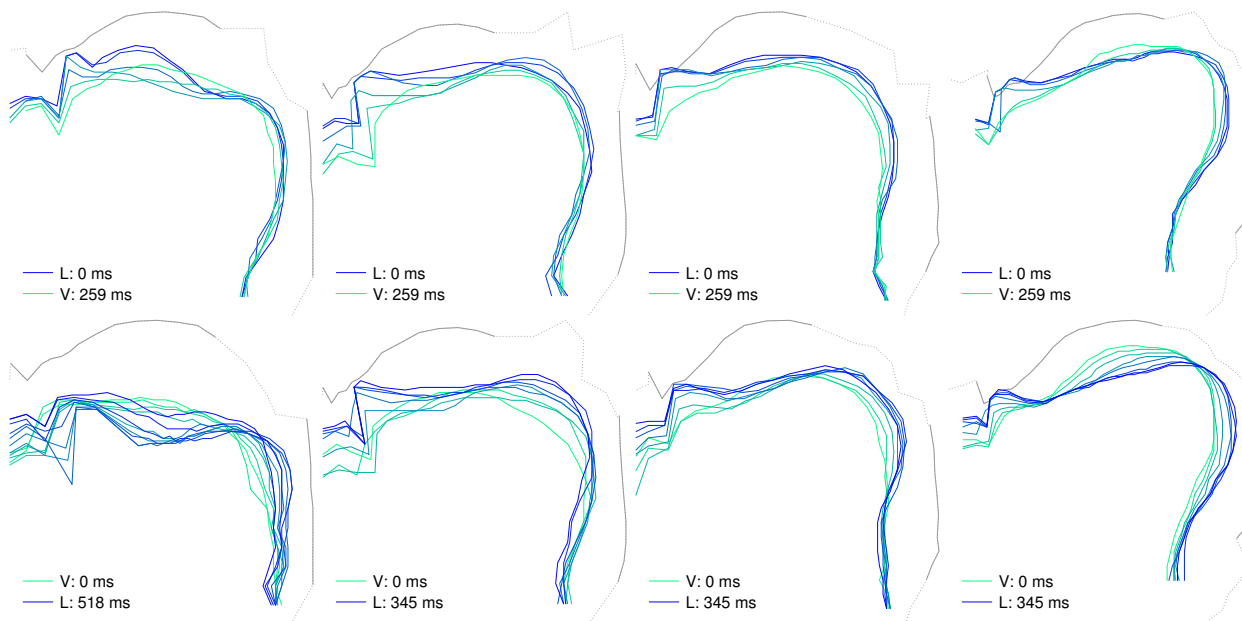


Figure 10: **Lateral Production in Mid Front Vowel Context.** Top row: onset (*'Lev'*); Bottom row: coda (*'bell'*); Left-to-right: W1, W2, W3, M1; Blue lines: tongue posture at lateral coronal target; Green lines: vowel target posture. Intermediate colors: tongue postures captured at 43 ms intervals in the transition between lateral and vowel.

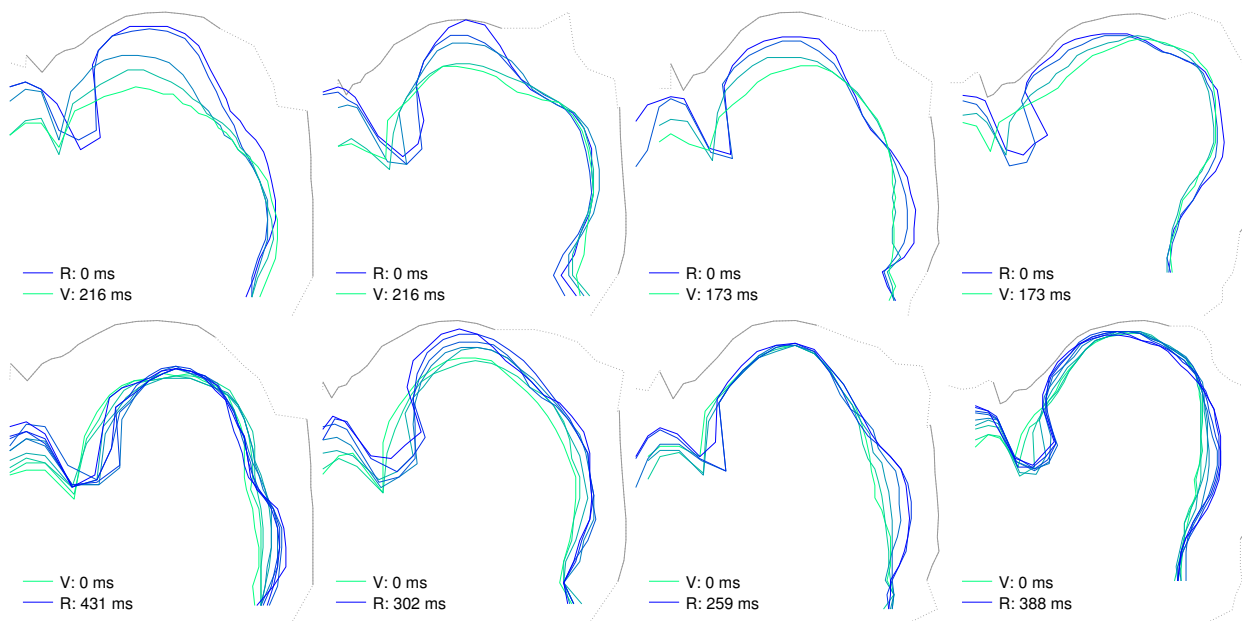


Figure 11: **Rhotic Production in Mid Front Vowel Context.** Top row: onset (*'rep'*); Bottom row: coda (*'bare'*); Left-to-right: W1, W2, W3, M1; Blue lines: tongue posture at rhotic coronal target; Green lines: vowel target posture. Intermediate colors: tongue postures captured at 43 ms intervals in the transition between rhotic and vowel.

1063
 1064
 1065
 1066
 1067
 1068
 1069
 1070
 1071
 1072
 1073
 1074
 360
 1075
 1076
 1077
 1078
 1079
 1080
 1081
 365
 1082
 1083
 1084
 1085
 1086
 1087
 1088
 1089
 1090
 1091
 1092
 1093
 1094
 1095
 1096
 1097
 1098
 1099
 1100
 1101
 1102
 1103
 1104
 1105
 1106
 1107
 1108
 1109
 1110
 1111
 370
 1112
 1113
 1114
 1115
 1116
 1117
 1118
 1119
 1120
 1121

Liquid Articulation in Low Vowel Contexts. Lateral production in a low vowel context (/a/) is illustrated in Fig. 12. Individual variability can be observed in the height of the dorsum at the vowel target – W2, in particular, shows a higher dorsal posture at the start of the vowel – but all speakers produce this vowel with retraction/lowering of the back of the tongue into the pharynx, and lowering of the whole front of the tongue to create a large cavity under the palate. In comparison to laterals produced adjacent to front vowels, there is much less movement of the back of the tongue, both in the transition from onset [l] into the vowel (*‘lob’*), or from the vowel into the coda lateral (*‘ball’*). For speaker M1, the entire back of the tongue – from the root to the blade – remains stationary throughout the [aɫ] rime (Fig. 12, bottom right). For all speakers, there is very little displacement of the tongue root and the back of the tongue in the mid-pharyngeal region, either in onset or coda, despite the large amount of the coronal movement, and despite the fact that these sequences begin at the coronal target, which is more peripheral to the nucleus than the dorsal context in all cases (Table 3). This suggests that the intrinsic dorsal target of the lateral is very similar to that of /a/, and/or the lateral dorsal gesture is highly coarticulated with this vowel.

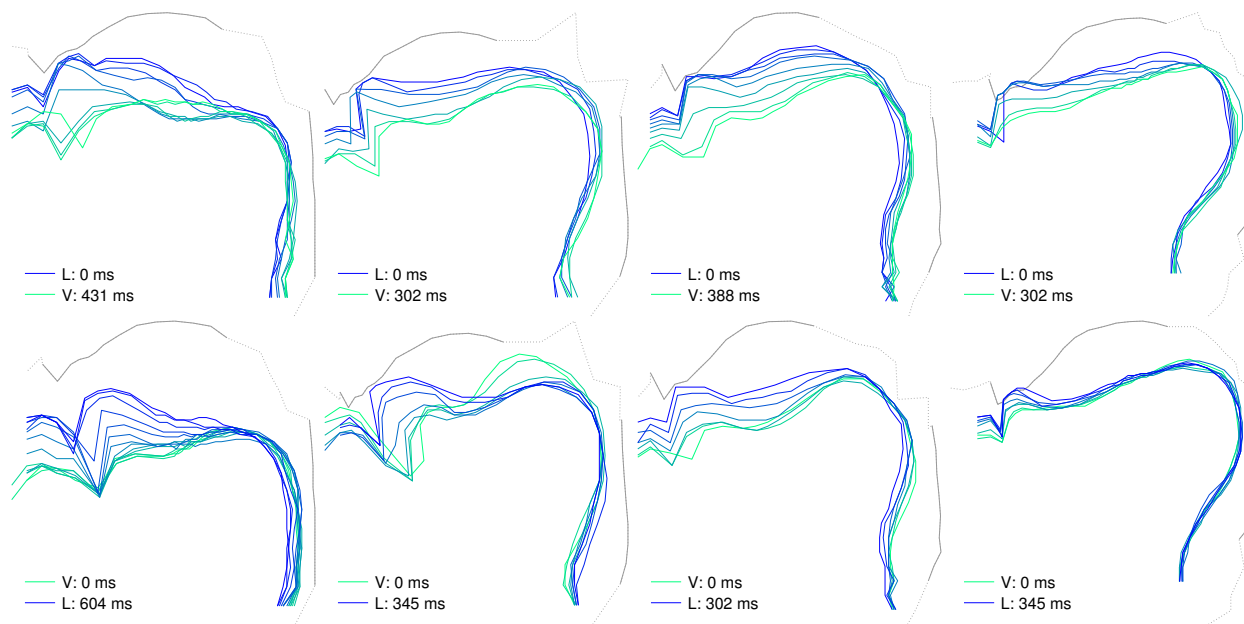


Figure 12: **Lateral Production in Low Vowel Context.** Top row: onset (*‘lob’*); Bottom row: coda (*‘ball’*); Left-to-right: W1, W2, W3, M1; Blue lines: tongue posture at lateral coronal target; Green lines: vowel target posture. Intermediate colors: tongue postures captured at 43 ms intervals in the transition between lateral and vowel.

Rhotics produced before and after the low vowel /a/ are compared in Fig. 13. In this vowel context, rhotics produced by all speakers show high stability in the tongue root and tongue back in onset position (*‘rob’*), where coronal and dorsal gestures are synchronous or near-synchronous (Table 4). Word-finally (*‘bar’*), where the rhotic dorsal gesture precedes the coronal gesture, more lingual displacement can be seen in the pharynx (Fig. 13, bottom row), in the transition from the nucleus to coda. In both syllable positions,

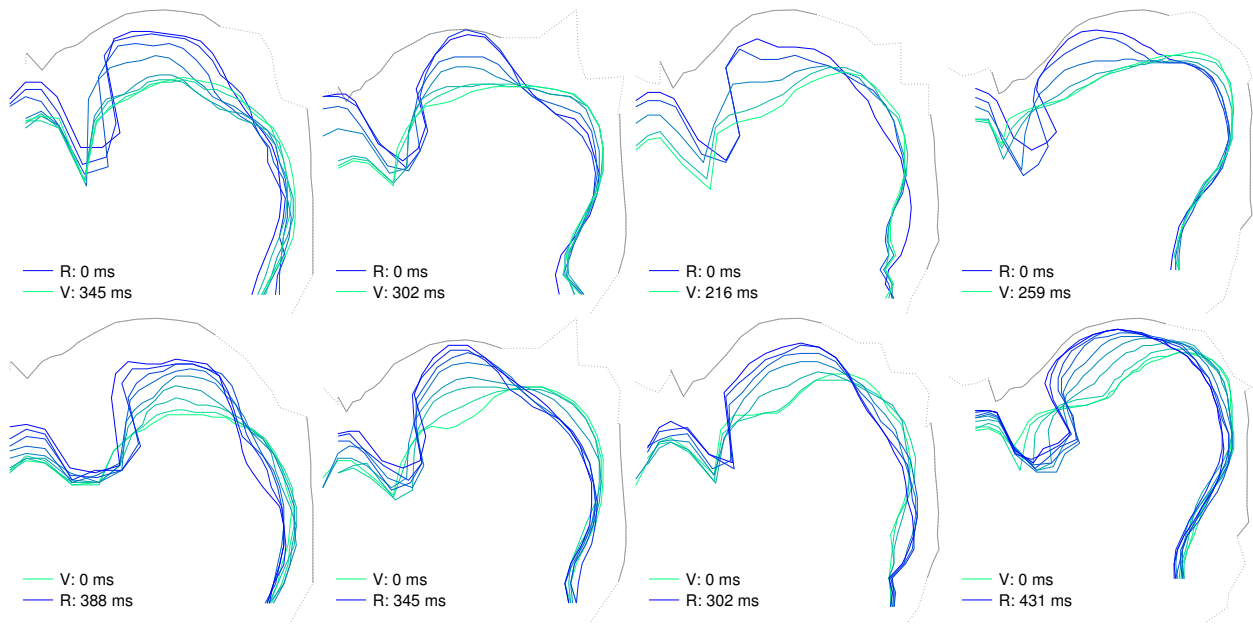


Figure 13: **Rhotic Production in Low Vowel Context.** Top row: onset (*'rob'*); Bottom row: coda (*'bar'*); Left-to-right: W1, W2, W3, M1; Blue lines: tongue posture at rhotic coronal target; Green lines: vowel target posture. Intermediate colors: tongue postures captured at 43 ms intervals in the transition between rhotic and vowel.

rhotics produced by all speakers in the low vowel context are characterized by large amounts of movement of the entire front part of the tongue towards or from the palatal approximant target. Speaker W3 shows the greatest asymmetry between $[-aɪ]$ and $[ɪa-]$, which is slightly retroflexed at the coronal target; but all speakers use the same global tongue shape for rhotics produced at both syllable margins. Similar patterns of articulation to those illustrated in Figs. 12–13 are also observed for liquids produced in $/\Delta/$ (*'love'*, *'mull'*, *'rum'*) contexts.

Liquid Articulation in Back Vowel Contexts. Laterals produced before and after $/oʊ/$ are compared in Fig. 14. As in the low vowel context, coda laterals produced by all speakers are characterized by high stability across the entire back of the tongue, from the root to the top of the dorsum. For all speakers, the onset in *'lobe'* is less articulatorily similar to $[oʊ]$ than the coda allophones following the same vowel (*'pole'*). As in the low vowel context, onset laterals are produced with the tongue blade and the front of the dorsum raised and less concave than the coda variants in *'pole'*. Onset/coda lateral asymmetries are especially pronounced for M1, who has a high back initial vocalic target for $[oʊ]$ in *'lobe'*, requiring raising and backing of the entire tongue body from the mid-pharyngeal target of the initial lateral. In contrast, M1's coda lateral following the same vowel is produced with virtually no movement from the preceding $[oʊ]$ (Fig. 14, bottom right panel), maintaining the same global tongue posture throughout the entire rime of *'pole'*.

1181
 1182
 1183
 1184
 1185
 1186
 1187
 1188
 1189
 1190
 1191
 1192
 1193
 1194
 1195
 1196
 1197
 1198
 1199
 1200
 1201
 1202
 1203
 1204
 1205
 1206
 1207
 1208
 1209
 1210
 1211
 1212
 1213
 1214
 1215
 1216
 1217
 1218
 1219
 1220
 1221
 1222
 1223
 1224
 1225
 1226
 1227
 1228
 1229
 1230
 1231
 1232
 1233
 1234
 1235
 1236
 1237
 1238
 1239

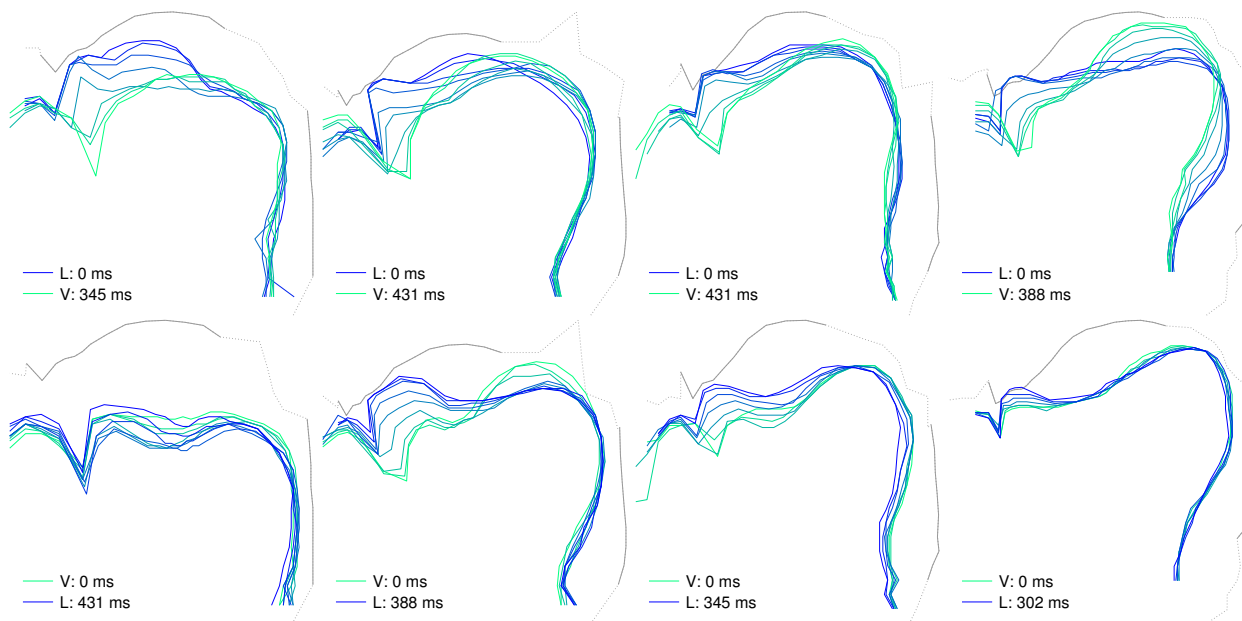


Figure 14: **Lateral Production in Back Vowel Context.** Top row: onset (*'lobe'*); Bottom row: coda (*'pole'*); Left-to-right: W1, W2, W3, M1; Blue lines: tongue posture at lateral coronal target; Green lines: vowel target posture. Intermediate colors: tongue postures captured at 43 ms intervals in the transition between lateral and vowel.

Fig. 15 compares rhotics produced before and after the back vowel /*ou*/. Unlike laterals produced in back vowel contexts, all rhotics show displacement of the back of the tongue in the transition to (*'robe'*) or from (*'bore'*) the vowel target. At both syllable margins, rhotics are produced with a constriction in the lower (W1, W3), mid (W2) or upper (M1) pharynx that differs from the pharyngeal posture at the vowel target. The saddle formed in the middle of the tongue between coronal and dorsal constrictions at the [ɹ] target is especially notable in rhotic production sequences in back vowel contexts because it coincides with the vowel constriction location. /*ouɹ*/ rimes are articulated by lowering of the tongue from a vowel target constriction formed with a monolithic bunched gesture of the whole tongue, and creation of separate constrictions in the pharynx and the palate (Fig. 15, bottom row). Similar patterns of articulation to those illustrated in Figs. 14–15 are observed for liquids produced in /*ʊ*/ (*'loof'*, *'pull'*, *'boor'*), and /*u*/ (*'loop'*, *'pool'*, *'rube'*) contexts.

3.5. Coarticulatory Resistance of Liquid Consonants

Articulatory target postures were compared for liquid consonants produced in different vowel contexts, using the method illustrated in Fig. 4. Mean lingual displacement across 30 laterals and 30 rhotics produced by each speaker are compared in Table 5. Each cell shows mean displacement within a set of 15 tongue outlines from the mean lingual posture calculated over that set. For each liquid at each syllable margin, mean displacement was calculated at the dorsal target of the consonant, in two different coarticulatory

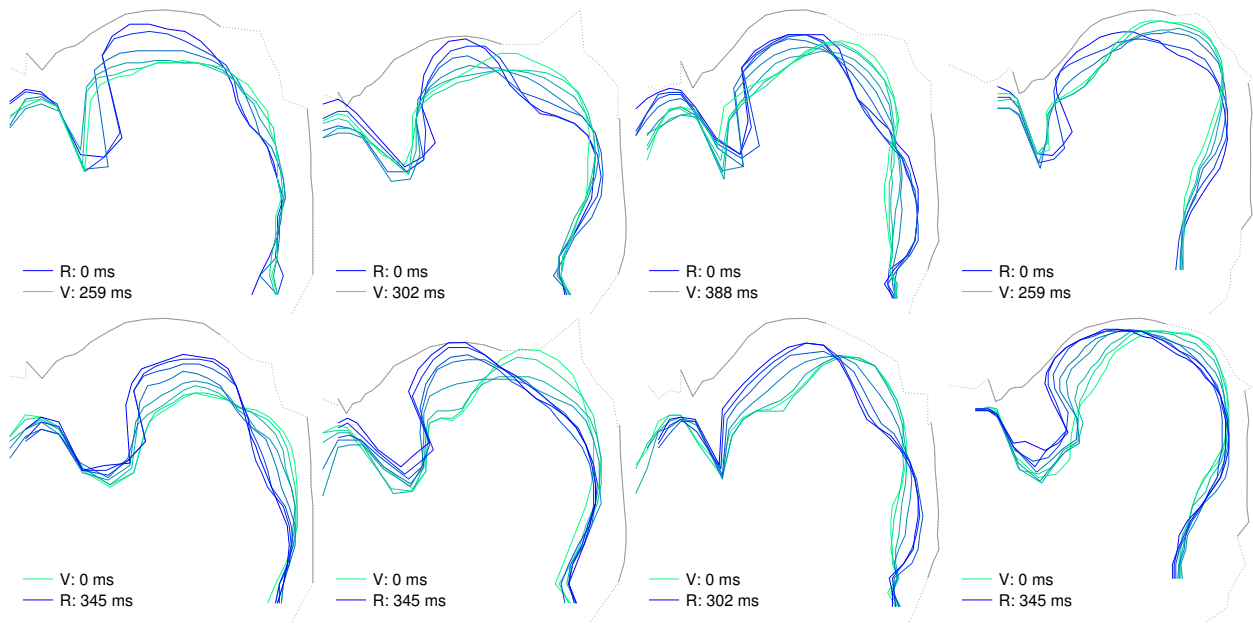


Figure 15: **Rhotic Production in Back Vowel Context.** Top row: onset (*'robe'*); Bottom row: coda (*'bore'*); Left-to-right: W1, W2, W3, M1; Blue lines: tongue posture at rhotic coronal target; Green lines: vowel target posture. Intermediate colors: tongue postures captured at 43 ms intervals in the transition between rhotic and vowel.

environments: adjacent to a set that we labeled 'tense' vowels [i-ei-ɑ-o-u], and a set that we labeled 'lax' vowels [ɪ-ɛ-ɑ-o-u]. Each comparison was made within one of the (partially overlapping) sets of five vowels that can appear (and neutralize) before a coda rhotic, so that estimates of coarticulatory resistance were balanced in the number of tokens and the range of vowel qualities influencing articulation of the target liquid over the entire vowel space. To balance the sets, it was necessary to include the low back vowel and the mid back round vowel in both groups. As discussed in Section 2.2, in pre-lateral and pre-rhotic contexts, the mid back round vowel may be realized as [o(u)] or [ɔ], depending on speaker and context. For Speaker W1, for example, the 15 onset laterals occurring before tense vowels (3 repetitions each of *'leap'*, *'lame'*, *'lob'*, *'lobe'*, *'loop'*) were displaced from the mean midsagittal posture of the set by an average of 2.8 mm (per analysis gridline), over the length of the tongue from the sublingual cavity to the base of the epiglottis (Table 5, top left).

Word-initial liquids vary in their resistance to coarticulatory influence by neighboring vowels. W3's onset laterals are more resistant to coarticulation before both tense and lax vowels than her onset rhotics (Table 5, row 3). For the other three participants, onset rhotics are produced with less displacement from mean lingual posture than onset laterals in each set of vowel contexts. For all four speakers, coda rhotics are less displaced from their common posture at the dorsal target than laterals produced after the equivalent vowels (Fig. 16).

1299
 1300
 1301
 1302
 1303
 1304
 1305
 1306
 1307
 1308
 1309
 1310
 1311
 1312
 1313
 1314
 1315
 1316
 1317
 1318
 1319
 1320
 1321
 1322
 1323
 1324
 1325
 1326
 1327
 1328
 1329
 1330
 1331
 1332
 1333
 1334
 1335
 1336
 1337
 1338
 1339
 1340
 1341
 1342
 1343
 1344
 1345
 1346
 1347
 1348
 1349
 1350
 1351
 1352
 1353
 1354
 1355
 1356
 1357

Table 5: **Mean Lingual Displacement due to Coarticulatory Influence of Adjacent Vowels.** Mean total displacement (s.d.) in mm/gridline from mean posture at dorsal target of liquid.

| | VOWEL SET | ONSET | | CODA | |
|------|--------------|-----------|-----------|-----------|-----------|
| | | LATERAL | RHOTIC | LATERAL | RHOTIC |
| W1 | [i-eɪ-ɑ-o-u] | 2.8 (1.1) | 1.5 (0.4) | 2.1 (0.9) | 1.4 (0.4) |
| | [ɪ-ɛ-ɑ-o-ʊ] | 2.6 (0.9) | 1.5 (0.4) | 1.9 (0.6) | |
| W2 | [i-eɪ-ɑ-o-u] | 1.4 (0.4) | 1.1 (0.3) | 2.4 (0.8) | 1.0 (0.2) |
| | [ɪ-ɛ-ɑ-o-ʊ] | 1.4 (0.5) | 1.1 (0.1) | 2.2 (0.6) | |
| W3 | [i-eɪ-ɑ-o-u] | 1.3 (0.5) | 1.6 (0.4) | 2.5 (0.9) | 1.8 (0.3) |
| | [ɪ-ɛ-ɑ-o-ʊ] | 1.1 (0.3) | 1.4 (0.5) | 2.3 (0.9) | |
| M1 | [i-eɪ-ɑ-o-u] | 1.9 (0.6) | 1.2 (0.3) | 1.5 (0.4) | 1.1 (0.4) |
| | [ɪ-ɛ-ɑ-o-ʊ] | 1.8 (0.6) | 1.3 (0.3) | 1.4 (0.4) | |
| Mean | | 1.8 (0.6) | 1.3 (0.2) | 2.0 (0.4) | 1.3 (0.3) |

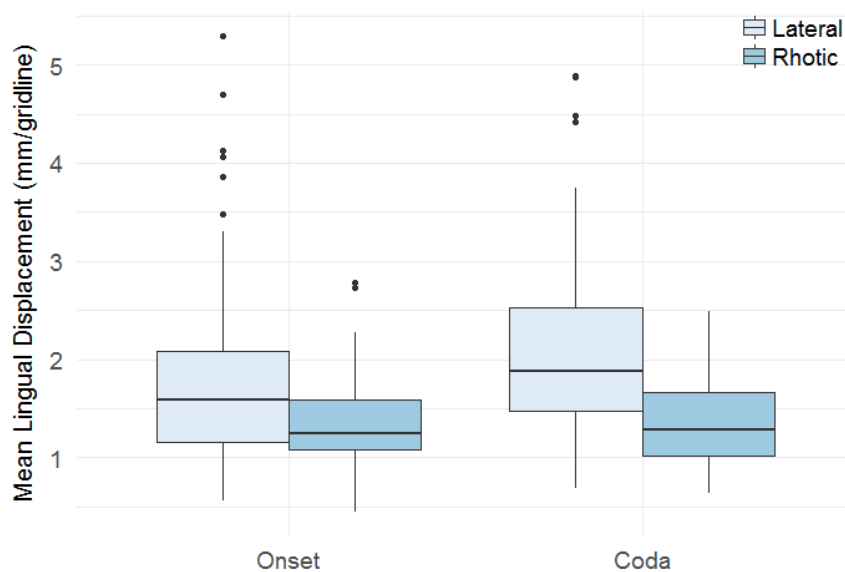


Figure 16: **Mean Lingual Displacement at Liquid Dorsal Target.** Mean displacement (mm/gridline), all speakers: 120 word-initial laterals vs. 120 word-initial rhotics; 120 word-final laterals vs. 120 word-final rhotics.

1358
1359
1360
1361
1362
1363
1364
1365
1366
1367
1368
1369
1370
1371
1372
1373
1374
1375
1376
1377
1378
1379
1380
1381
1382
1383
1384
1385
1386
1387
1388
1389
1390
1391
1392
1393
1394
1395
1396
1397
1398
1399
1400
1401
1402
1403
1404
1405
1406
1407
1408
1409
1410
1411
1412
1413
1414
1415
1416

425 A linear mixed model was constructed to examine the interaction of liquid type and position on lingual displacement due to vocalic coarticulation. Log lingual displacement (mm/gridline) was modelled as a function of consonant and syllable position with random effects for speaker. A model including by-speaker random slopes for consonant and position provided a better fit to the data compared to the model with random intercepts only ($\chi^2(1) = 103$, $p < 0.001$). Consonant type was treatment coded as LATERAL = 0; RHOTIC = 1. Syllable Position was coded as CODA = 0; ONSET = 1 (details in Table C1). Rhotics were displaced less than laterals ($\beta = -0.41$, $t(3.4) = -3.3$, $p = 0.037$; $d = -0.85$, POWER = 46.2%), and there was an interaction between consonant and position, with liquids displaced less in onsets ($\beta = 0.19$, $t(467) = 3.39$, $p = 0.0008$; $d = 0.39$, POWER = 91.5%). Type III ANOVA of the model with Satterthwaite's method shows a main interaction between consonant and position ($F(1, 467) = 11.5$, $p = 0.0008$) and a smaller effect of consonant ($F(1, 3) = 7.1$, $p = 0.076$). These results should be interpreted with caution, given the sparsity of data per speaker due to the aggregated metric used to quantify lingual displacement: the data are underpowered with respect to the overall effect of consonant, but well powered with respect to the interaction between consonant and position.

Bearing in mind these caveats, these data are consistent with the hypothesis that rhotics are produced with more consistent tongue shaping than laterals, while also revealing that individual speakers differ in the ways that vowels and liquids interact. Greater differences between liquids are observed in codas, and the data in Table 5 reflect different types of coarticulatory behavior in coda liquids. Articulatory variability can be seen across the whole length of the tongue in the word-final laterals produced by speakers W1 and W2 (Fig. 17, left-most panels). Coda laterals vary most across vowel contexts for W3, but the back of her tongue body remains relatively stable compared to the greater displacement of the tongue tip and blade between tokens (Fig. 17, 3rd panel). M1's word-final laterals show the least variability at the dorsal target, primarily varying in the height of the top part of the dorsum (Fig. 17, right-most panel). Coda laterals produced by all four speakers are characterized by a region of local maximal coarticulatory variability at the tongue tip, which increases with the overall degree of lateral vocalization.

Speakers W2 and M1 show the greatest consistency in production of word final rhotics (Fig. 18: panels 2 and 4). Coda rhotics of both speakers are highly stable at the back of the tongue, with very little variability across vowel contexts from the tongue root to the front part of the dorsum. Coda rhotics varied most across vowel contexts for W3, followed by W1 (Table 5, last column). The majority of this variability arises from differences in articulation of the saddle between the coronal and dorsal constrictions, and in the height and degree of fronting of the coronal gesture (Fig. 18, 1st and 3rd panels). Compared to the coda laterals, word-final rhotics are characterized by much less coronal coarticulatory variability. No speaker's coda rhotics vary more than 8 mm (max. Euclidean displacement) in tongue tip posture at the dorsal target (W3: 'bar' vs. 'beer'), whereas coda laterals differ as much as 18 mm in tongue tip articulation across tokens produced after different vowels (W1: 'pill' vs. 'pull').

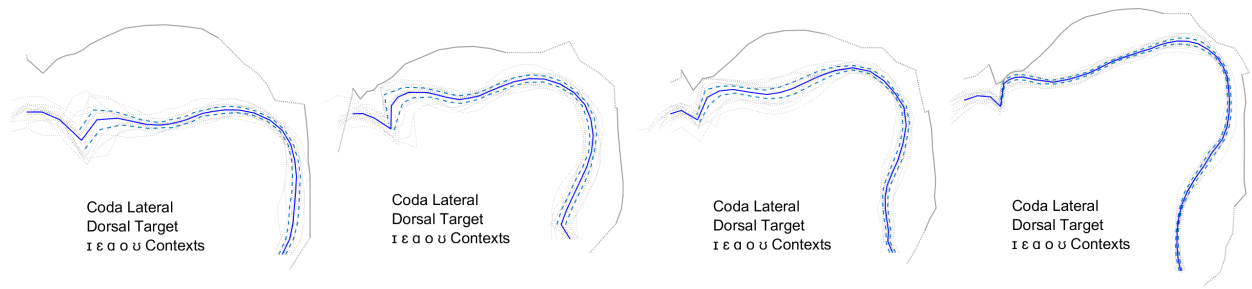


Figure 17: **Articular Variability in Coda Laterals.** Midsagittal tongue posture in 15 word-final laterals: 3 repetitions each of ‘pill’, ‘bell’, ‘ball’, ‘pole’, and ‘pull’. Left-to-right: Subjects W1, W2, W3, M1; Grey lines: lateral posture captured at dorsal target in each token; Blue solid lines: mean coda lateral tongue posture; Blue dashed lines: 2 s.d. from mean posture.

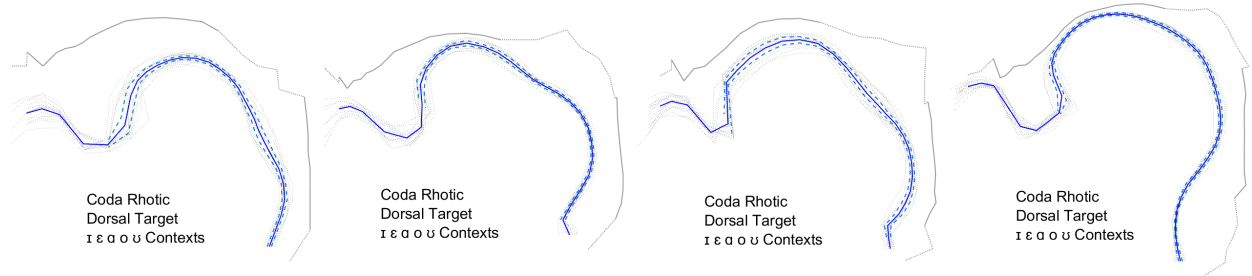


Figure 18: **Articular Variability in Coda Rhotics.** Midsagittal tongue posture in 15 word-final rhotics: 3 repetitions each of ‘beer’, ‘bare’, ‘bar’, ‘bore’, and ‘boor’. Left-to-right: Subjects W1, W2, W3, M1; Grey lines: rhotic posture captured at dorsal target in each token; Blue solid lines: mean coda rhotic tongue posture; Blue dashed lines: 2 s.d. from mean posture.

3.6. *Coarticulatory Influence of Liquid Consonants*

The influence of onset liquids on five different vowels is compared in Table 6. Each value – calculated using the method illustrated in Fig. 3 – indicates total lingual displacement (mm/gridline) from intrinsic vowel posture (captured in an inter-labial environment), in vowels produced after each consonant. Lingual displacement is calculated for each vowel which appears before coda rhotics (the most restricted environment: Table 2), allowing for direct comparison of both liquids in each syllable margin. Because these five vowel qualities are articulatorily dispersed throughout the vowel space, the mean values tabulated in the bottom row of each table therefore provide an estimate of the overall coarticulatory influence of each liquid on tautosyllabic vowels.

The influence of coda liquids on preceding vowels is compared using the same metric in Table 7. Each cell compares mean tongue posture at the target frame of a vowel in a liquid-final rime with the mean posture of the reference vowel repeated between two labial consonants, and indicates the total displacement (mm/gridline) between the two midsagittal lingual outlines. For speaker W1, for example, the mean vowel shape at the nucleus of ‘pill’ is displaced 0.4 mm/gridline from the target tongue posture in ‘bib’ (Table

Table 6: **Vocalic Deformation (mm/gridline) due to Coarticulatory Influence of Onset Liquids**

| | LATERAL | | | | RHOTIC | | | | |
|--------|---------|-----|-----|-----|--------|-----|-----|-----|-----|
| | W1 | W2 | W3 | M1 | W1 | W2 | W3 | M1 | |
| [lɪ-] | 0.7 | 0.8 | 0.6 | 0.6 | [ɪɪ-] | 0.6 | 0.8 | 0.8 | 0.5 |
| [lɛ-] | 1.1 | 0.5 | 0.4 | 0.4 | [ɛɛ-] | 0.6 | 0.6 | 0.3 | 0.3 |
| [lɑ-] | 0.4 | 0.8 | 0.2 | 0.6 | [ɪɑ-] | 0.7 | 0.6 | 0.2 | 0.3 |
| [loʊ-] | 0.6 | 0.6 | 0.9 | 0.5 | [ɪoʊ-] | 0.8 | 0.6 | 0.8 | 0.5 |
| [lʊ-] | 0.6 | 0.6 | 0.5 | 0.5 | [ɪʊ-] | 1.5 | 1.1 | 1.3 | 1.0 |
| Mean | 0.7 | 0.7 | 0.7 | 0.5 | Mean | 0.8 | 0.7 | 0.7 | 0.5 |

7, top left), while the tongue is displaced 1.1 mm/gridline from the reference interlabial vowel posture in the equivalent vowel before a coda rhotic in the word ‘beer’. Our choice of comparison vowel in interlabial context is the set [ɪ-ɛ-ɑ-o-ʊ], because the coarticulatory aggression data show that pre-coda vowels were less displaced from the un-coarticulated lax vowel set compared to the tense vowel comparisons (Table 5). The quality of vowels appearing before coda rhotics is not always clear, since tense/lax contrasts are neutralized in this environment. Nevertheless, we have good reason to believe that in the dialect of the study participants, as for most speakers of General American English, a non-diphthongal variant occurs in this environment (not [eɪ], [oʊ], [iʲ], or [uʷ]), and that the reference vowels are sufficiently close to those before /ɹ/ to make a valid basis of comparison.

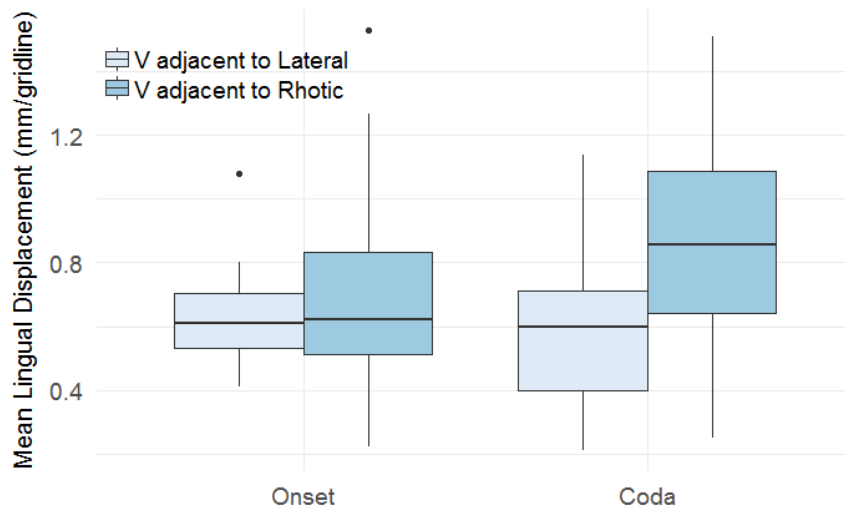
Table 7: **Vocalic Deformation (mm/gridline) due to Coarticulatory Influence of Coda Liquids**

| | LATERAL | | | | RHOTIC | | | | |
|-------|---------|-----|-----|-----|--------|-----|-----|-----|-----|
| | W1 | W2 | W3 | M1 | W1 | W2 | W3 | M1 | |
| [-ɪɪ] | 0.4 | 0.6 | 0.4 | 0.7 | [-ɪɪ] | 1.1 | 0.8 | 0.4 | 0.6 |
| [-ɛɪ] | 0.4 | 0.6 | 0.2 | 0.6 | [-ɛɪ] | 1.3 | 0.6 | 0.9 | 1.0 |
| [-ɑɪ] | 0.4 | 0.8 | 0.3 | 0.6 | [-ɑɪ] | 0.6 | 0.8 | 0.4 | 0.8 |
| [-oɪ] | 0.7 | 0.8 | 0.4 | 1.1 | [-oɪ] | 1.0 | 1.0 | 0.2 | 1.1 |
| [-ʊɪ] | 0.7 | 0.6 | 0.6 | 0.8 | [-ʊɪ] | 1.5 | 1.8 | 0.5 | 1.5 |
| Mean | 0.5 | 0.7 | 0.4 | 0.7 | Mean | 1.1 | 0.9 | 0.5 | 1.0 |

A linear mixed model was constructed to examine the interaction of liquid type and position on lingual displacement in vowels. Vocalic deformation (mm/gridline) was modelled as a function of consonant and

1535
 1536
 1537
 1538
 1539
 1540
 1541 485 syllable position with random effects for speaker. A model including by-speaker random slopes for posi-
 1542 tion provided a better fit to the data compared to the model with random intercepts only ($\chi^2(1) = 6.7$,
 1543 $p = 0.03$). Consonant type was treatment coded as LATERAL = 0; RHOTIC = 1. Syllable Position was coded
 1544 as CODA = 0; ONSET = 1 (details in Table C2). Rhotics had a greater effect on vowel displacement than later-
 1545 als ($\beta = 0.29$, $t(70) = 3.73$, $p < 0.001$; $d = 0.90$, POWER = 89.8%), and the effect of consonant was greater in
 1546 coda position ($\beta = 0.22$, $t(70) = 1.98$, $p = 0.051$; $d = 0.68$, POWER = 50.6%). Type III ANOVA of the model
 1547 490 with Satterthwaite's method shows a main effect of consonant ($F(1, 70) = 10.8$, $p = 0.002$) and a smaller
 1548 interaction between consonant and position ($F(1, 70) = 3.95$, $p = 0.051$). These results should be interpreted
 1549 with caution, given the sparsity of data per speaker due to the aggregated metric used to quantify vocalic
 1550 deformation: the data are underpowered with respect to the interaction between consonant and position,
 1551 but well powered with respect to the overall effect of consonant on vowel articulation.
 1552
 1553
 1554 495

1555 Bearing in mind these caveats, these data suggest that overall for these four speakers, coda rhotics have
 1556 a greater influence on a vowel in the same syllable than both onset rhotics and onset laterals; however, the
 1557 relative influence of liquids on a specific vowel also varies across speakers. In particular, there is greater
 1558 deformation of pre-lateral vowels compared to pre-rhotic equivalents for W3 'pole' > 'bore', W3 'pull' > 'boor',
 1559 and M1 'pill' > 'beer'. For all other rimes, a coda rhotic has the same or more influence on the preceding
 1560 500 vowel than a lateral (Fig. 19).
 1561
 1562
 1563
 1564



1565
 1566
 1567
 1568
 1569
 1570
 1571
 1572
 1573
 1574
 1575
 1576
 1577
 1578
 1579
 1580
 1581
 1582
 1583
 1584
 1585
 1586
 1587
 1588
 1589
 1590
 1591
 1592
 1593

Figure 19: **Mean Lingual Displacement at Vowel Target from Default Vowel Posture: lax vowels adjacent to Liquids.** Mean lingual posture of vowels produced after/before liquid consonants (three repetitions of each of five vowels), compared to mean posture of same vowels produced in inter-labial contexts (two repetitions). Euclidean distances between two tongue shapes calculated from tongue root to sub-lingual cavity, averaged across all speakers (mm/grid line).

1594
1595
1596
1597
1598
1599
1600 *3.7. Summary of Main Findings*

1601 Midsagittal articulation of rhotic and lateral approximants by four speakers was compared in all phono-
1602 tactic environments where liquid consonants occur in General American English syllables with simple mar-
1603 gins. The main findings of this study, with respect to intergestural coordination, are:
505

- 1605 i. in **onset laterals**, the coronal gesture was achieved before the dorsal gesture reached its target in all
1606 vowel contexts; maximum TB retraction was achieved, on average, 190 ms after TT closure/maximum
1607 advancement
1608
- 1609 ii. lingual gestures were sequenced in the reverse order in **coda laterals**, but complete midsagittal tongue
1610 tip closure was only observed in 54% of 120 lateral-final words; maximum TB retraction was achieved
510 1611 approximately 150 ms before TT closure/maximum advancement
1612
- 1613 iii. **onset rhotics** were produced with synchronous coronal and dorsal gestures, preceded by labial ap-
1614 proximation/protrusion (mean 20 ms before the lingual gestures)
1615
- 1616 iv. in **coda rhotics**, the posterior lingual gesture preceded the coronal gesture by 80 ms (mean across all
1617 vowel contexts); no evidence of a labial gesture was found in word-final rhotics
515 1618

1619
1620 The main findings of this study, with respect to patterns of liquid co-production, are:

- 1621 i. rhotics showed greater **consistency in target posture** across syllable positions than laterals, which
1622 displayed greater articulatory differences between onset and coda variants
1623
- 1624 ii. rhotics showed greater **resistance to coarticulation** across vowel contexts than laterals: lingual
1625 displacement from mean posture was significantly lower for rhotics compared to laterals at both syllable
520 1626 margins
1627
- 1628 iii. vowels adjacent to rhotics were significantly more displaced from construed target postures than when
1629 produced adjacent to laterals. Coda rhotics induced greater displacement, consistent with exertion of
1630 the greatest **coarticulatory influence** on tautosyllabic vowels
1631
1632
1633
1634
1635
1636
1637
1638
1639
1640
1641
1642
1643
1644
1645
1646
1647

1653
1654
1655
1656
1657
1658
525 **4. Discussion**
1659

1660 The articulatory characterization of liquids based on these data is broadly consistent with previous
1661 studies. However, some new insights emerge from the more complete picture of the vocal tract afforded by
1662 rtMRI, and from comparing the ways that liquids coarticulate in previously unexamined environments. The
1663 rtMRI data reveal the importance of studying liquid consonant production in a wide range of positional and
1664 vowel contexts, to more fully understand the interaction of the intrinsic gestures of the liquids with those
530 of the surrounding sounds, and how these may differ across individuals (see Mielke et al., 2016).
1666
1667
1668

1669
1670 *4.1. Characterizing Multigestural Segments*

1671 An important methodological insight reinforced by these data is that there is no single timepoint at which
1672 all phonetic features of laterals or rhotics can be robustly characterized or consistently compared across all
1673 contexts and speakers. Previous studies have reported key phonetic parameters of liquids captured at a
535 single point in time, assumed to be the consonantal target. All formant values in Bladon & Al Bamerni
1674 (1976), for example, were measured at “each occurrence of /l/” (p.139), and Giles & Moll (1975) compare
1675 allophonic variants of laterals from composite images acquired “during steady-state configurations ... in
1676 which the positions of both the tongue apex and dorsum were invariant” (p.210). These rtMRI data reveal
1677 that speakers rarely achieve articulatory steady states during liquid production, and that target consonantal
540 postures may not be directly comparable across speakers because of individual differences in realization and
1681 coordination. Even for onset rhotics – the liquid allophone in which lingual gestures are most consistently
1682 synchronized – a single target frame cannot be consistently identified because maximum labial approximation
1683 typically leads lingual accomplishment. Attempts to compare liquid parameters at a single goal – such as
1684 maximum lingual elongation – were therefore abandoned in this study in favor of separate analyses at coronal
545 and dorsal landmarks.
1688
1689

1690
1691 *4.2. Lateral Goals of Production*
1692

1693 Mean lateral tongue shapes for speakers M1, W3 and W2 (Fig. 6) closely resemble those of subjects A,
1694 B and C respectively, in the study by Giles & Moll (1975). All W1’s laterals, on the other hand, show the
1695 dorsum to be considerably lower than the tongue tip at the landmark of the coronal target, unlike the other
550 three speakers in this study and all speakers imaged by Giles & Moll (1975). Speaker JO in the ultrasound
1697 study of Lee-Kim et al. (2013) produces the laterals in ‘tallest’ and ‘flawless’ with a dorsum marginally
1698 lower than the tongue tip, but all other laterals in that six-speaker study appear to be articulated with the
1699 back of the tongue at least as high as the tongue tip.
1700

1701
1702
1703
555 Leidner (1976) observed in an electromyograph study of two speakers of American English that less muscle
1704 activity was involved in lateral production after back vowels compared to front vowels, and characterized the
1705 lateral dorsal target as [u]-like. The patterns of coda lateral production examined here are consistent with
1706
1707
1708
1709
1710
1711

1712
1713
1714
1715
1716
1717
1718
1719
1720
560 1721
1722
1723
1724
1725
1726
1727
565 1728
1729
1730

Leidner’s findings in that they generally demonstrate less tongue body retraction in back vowel contexts. Dorsal targets in laterals produced by W2 and W3’s closely resemble their [u] and [ʊ] vowels respectively, consistent with Leidner’s and other characterizations (e.g. Hardcastle & Barry’s (1989) study of lateral vocalization in Southern British English). However, these MRI data show that the exact target of the lateral posterior gesture is speaker-specific and cannot always be characterized as velar. In particular, the lateral tongue body constriction location for W1 is very much lower than her dorsal target for [u], and more closely matches her [a] (Fig. 12). M1’s laterals also have a dorsal target that is lower and more retracted than the other speakers, and appears to be closer to his [ʌ].

4.3. Rhotic Goals of Production

1731
1732
1733
1734
1735
570 1736
1737
1738
1739
1740
1741

The rhotics produced by all four speakers in this study have lingual postures which fit into established typologies of American English /ɹ/. In Delattre & Freeman’s (1968) classification, W3’s rhotic closely resembles Type 4, those produced by W1 and W2 match Types 5/6, and M1’s rhotic resembles Types 1 to 3, in terms of global shaping. The positional allophony observed in these MRI data is consistent with the findings of Hagiwara (1994) that speakers with ‘blade up’ initial rhotics typically realize syllabic and final /ɹ/ with ‘tip down’ – i.e. less retroflexed or more bunched – tongue postures. The more bunched and rounded postures of the coda rhotics in our study also closely resemble the cineradiographic tracings of post-vocalic [ɹ] presented in Lindau (1985).

1742
575 1743
1744
1745
1746
1747
1748
1749
580 1750
1751
1752
1753
1754
1755

Considerable interspeaker variability was observed in the location of the pharyngeal constriction for /ɹ/ in these data (Sec. 3.2). Similar variability can also be seen among Lindau’s six speakers of American English: the lowest constriction in that study was formed with the epiglottis in the lowest part of the pharynx (P5), at a similar location to W1’s coda rhotic (Fig. 7), and Lindau’s speakers P2, P3, and P6 all articulate the rhotic in ‘herd’ with a mid-pharyngeal TB constriction similar to that of W2. The primary posterior constriction of M1’s rhotic was strikingly high across both syllable positions and all vowel contexts: approximately 30 mm higher than the mid-pharyngeal constriction of W2, and closer to the uvular than the glottis. M1’s rhotic appears to have a pharyngeal constriction target located further from the glottis than that of most other American English speakers for which rich imaging data of the pharynx is available (Delattre & Freeman, 1968; Lindau, 1985; Alwan et al., 1997; Espy-Wilson et al., 2000; Zhou et al., 2008).

1756
585 1757
1758
1759
1760
1761
1762
1763
590 1764
1765
1766
1767
1768
1769
1770

Although some activity in the epiglottal region was observed during rhotic production by all speakers, neither M1 nor W2 has a rhotic in which the narrowest part of the pharyngeal constriction is formed with the tongue root (cf. Gick & Campbell, 2003). These data suggest that the posterior rhotic gesture is better characterized as dorsal: regardless of the specific constriction location, it is formed between the back of the tongue body and the rear pharyngeal wall (Alwan et al., 1997; Espy-Wilson et al., 2000). It should be noted again that all midsagittal lingual profiles in this study were traced along the back of the tongue inside the epiglottis for consistency across frames and speakers, so exact comparisons of articulation in the lower

1771
1772
1773
1774
1775
1776 pharyngeal region with x-ray, cineradiographic, and ultrasound studies that trace the lower dorsum outside
1777 the epiglottis are not always possible.
1778

1780 *4.4. Patterns of Coarticulation*

1781
1782 595 This study has revealed differences in the coarticulatory properties of liquids that may influence their
1783 phonological behavior. Rhotics were more resistant to coarticulatory influence than laterals at both syllable
1784 margins, but the contrast between coda consonants was greater in this respect (Fig. 16). In addition, rhotics
1785 were found to exert more coarticulatory influence on adjacent vowels, especially in codas (Fig. 19). These
1786 coarticulatory patterns are consistent with the predictions of our hypothesis that rhotics are represented
1787 with a dorsal gesture with a higher specified blending strength than that of laterals in General American
1788 English; however, these findings should be interpreted with caution, given the limited number of participants
1789 600 in this study.
1790
1791

1792 Since there is no tense-lax vowel contrast before coda rhotics, one possible account of these findings is that
1793 the differences in tongue shaping before rhotics arise because the vowel in this context is actually a different
1794 quality with a different articulatory target to the comparison vowel elicited in the labial coda context. This
1795 605 is a more extreme case of the general problem of categorizing and comparing vowel quality across different
1796 words and contexts: some vowel quality differences are also reduced in pre-lateral environments, for example,
1797 and there may be sound changes involving mergers of some pre-lateral vowel contrasts in progress for some
1798 speakers (Labov et al., 2005). Nevertheless, the metrics explored here offer useful insights into the relative
1799 coarticulatory influences of liquids in different positions because they make reference to the entire vowel
1800 space, rather than individual vowel qualities. Further evidence for the idea that rhotics are characterized by
1801 greater coarticulatory dominance than laterals comes from their behavior in onsets, where they were found
1802 to be more resistant to coarticulatory deformation than laterals (Section 3.5). Furthermore, although the
1803 610 differences in coarticulatory aggression between liquids were greatest in codas (based on the construed vowel
1804 targets), rhotics were also significantly more influential on adjacent vowel posture overall – i.e. across both
1805 syllable margins (Section 3.6). Collectively, this suggests that these data are not merely artifacts resulting
1806 from measuring vowels already neutralized to a different quality before coda rhotics.
1807
1808

1809 If these patterns hold for other speakers of American English, they may be factors in the restriction of
1810 vowel qualities before coda rhotics. Tense-lax contrasts, for example, may be harder to maintain in a pre-
1811 rhotic environment where the consonant exercises greater influence on the nuclear vowel. Coda laterals, if
1812 620 more adaptable and less coarticulatorily aggressive, would be more likely to support a greater variety of vowel
1813 qualities in their rimes, including fine contrasts. These data also shed more light on the question of vowel
1814 identity before coda rhotics (Giegerich, 1992; Hammond, 1999). The patterns of coarticulation observed here
1815 are consistent with the analysis of Kenyon & Knott (1953) and Wells (1982, 481-485), who argue that lax
1816 625 variants appear before rhotics in General American English. Vowels produced in this environment might be
1817
1818
1819
1820
1821
1822
1823
1824

1830
1831
1832
1833
1834
1835 more centralized if a following rhotic exerts greater influence on the tongue body, resisting vowel movement
1836 to more peripheral targets or to targets more displaced from the intrinsic dorsal posture associated with an
1837 individual speaker's rhotic.
1838

1839 This raises further questions about the broader mechanisms by which such intergestural relationships
1840 might condition vowel neutralization among individuals in a speech community. We are not committed to
1841 630 whether such neutralization phenomena are synchronic or diachronic, or both. Nevertheless, the patterns
1842 identified in Section 1 are systematic across the General American English lexicon. While a phonological
1843 analysis goes beyond the scope of this paper, we suggest that our phonetic investigation can provide insight
1844 into the gestural representation that gives rise to this pattern that could inform a phonological account.
1845 Walker & Proctor (2013) have described some phonological properties of rhotic-initial complex codas in
1846 635 General American English which may be influenced by articulatory properties of vowel-rhotic-consonant
1847 sequences.
1848
1849
1850
1851

1852 *4.5. Patterns of Gestural Coordination*

1853 The basic patterns of gestural coordination observed in these rtMRI data are largely consistent with
1854 640 those described in previous studies, however the magnitude and details of some intergestural timings differ.
1855 Gick & Campbell (2003) also reported a positive lag of similar magnitude (10-20 ms) between the labial and
1856 lingual gestures of initial rhotics produced by eight speakers of American and other varieties of English, but
1857 found the lingual (and labial) gestures of coda rhotics to be near-synchronous. A longer and more consistent
1858 lag between lingual gestures was observed in word-final rhotics in this study: the tongue body/root gesture
1859 645 preceded the anterior constriction by 80 ms on average. Gick et al. (2006) found no lag between the lingual
1860 gestures of Western Canadian laterals in both pre- and post-vocalic positions. Three key differences between
1861 these studies may account for these discrepancies. Final rhotics in this study were compared across a greater
1862 range of vowel contexts ([i-ε-α-o-ū] vs. [i-a]), our experimental corpus was elicited with single word utterances
1863 (rather than in a carrier phrase), and the locations at which lingual constrictions were measured differed.
1864 MRI more consistently reveals more of the lower pharynx than ultrasound, which allowed us to measure the
1865 650 posterior gesture of the rhotic closer to the tongue root, where articulation may vary from other regions at
1866 the back of the dorsum.
1867
1868
1869
1870
1871
1872
1873

1874 Inter-gestural timings in these data are also longer than those reported for Scottish and Southern British
1875 English laterals (Scobbie & Pouplier, 2010). Mean lag between achievement of alveolar constriction and
1876 655 beginning of dorsal retraction in that study did not exceed 66 ms word-initially, and 126 ms for word-final
1877 laterals. Methodological differences would also appear to be the most likely cause of this discrepancy.
1878 Different gestural landmarks were used in Scobbie & Pouplier's study, and timing data were determined
1879 from patterns of EPG contact which indirectly gauge tongue body retraction, and may not be directly
1880 comparable with rtMRI measurements tracking tissue boundaries. Most importantly, those laterals were
1881
1882
1883

1889
 1890
 1891
 1892
 1893
 1894
 1895
 1896
 1897
 1898
 1899
 1900
 1901
 1902
 1903
 1904
 1905
 1906
 1907
 1908
 1909
 1910
 1911
 1912
 1913
 1914
 1915
 1916
 1917
 1918
 1919
 1920
 1921
 1922
 1923
 1924
 1925
 1926
 1927
 1928
 1929
 1930
 1931
 1932
 1933
 1934
 1935
 1936
 1937
 1938
 1939
 1940
 1941
 1942
 1943
 1944
 1945
 1946
 1947

660 elicited in full sentences, which will shorten timings compared to the longer durations of the isolated word utterances we used in this study.

Furthermore, when we consider only the intergestural timings of laterals elicited in the most comparable vowel context to that used in Scobbie & Pouplier (2010) – ‘*leap*’-‘*peel*’ – we find similar lags for some speakers, and variability that reflects individual speaker differences in lateral articulation. W1 has a much longer mean coda lateral lag (TT–TB = 273 ms) in high front vowel contexts than the other three speakers (mean 67 ms), which may result in part from her more retracted lateral dorsal target. For this speaker, lateralization of the tongue in the rime of ‘*peal*’ requires greater dorsal excursion from the palatal target of the nucleus towards an [a]-like target, compared to higher, fronter lateral dorsal targets of the other speakers in this study.

670 4.6. Patterns of Vowel-Liquid Interaction

A motivating goal of this study was to shed more light on asymmetries in the ways that liquids restrict and interact with vowels in English rimes. To facilitate examination of these issues, mean lags between lingual gestures for both liquids have been recalculated from Tables 3–4 and plotted together in Fig. 20 for comparison. Laterals at both syllable margins show greater mean temporal displacement between achievement of coronal and dorsal goals compared to rhotics produced in the same positions. This greater intergestural lag means that more time is available for articulators to move between tasks. The phonetic basis for this lag difference remains an open question. One possibility is that laterals and rhotics might differ in the relative independence of their coronal and dorsal gestures in temporal and/or spatial dimensions.

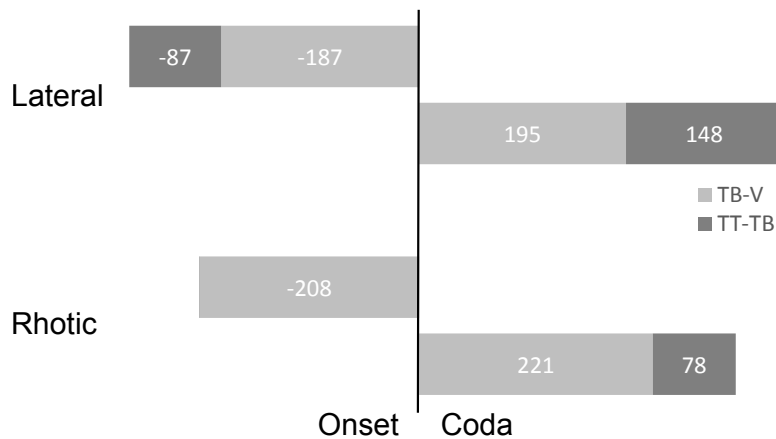


Figure 20: **Mean Lags between Lingual Gestures.** Mean lags (ms, all speakers) between achievement of coronal and dorsal gestures (TT–TB), and dorsal and vowel gestures (TB–V). Negative lags (left): intergestural timing for onset liquids; Positive lags (right): intergestural timing for coda liquids. TT–TB lag is zero for onset rhotics.

1948
1949
1950
1951
1952
1953
1954
1955
1956
1957
1958
1959
1960
1961
1962
1963
1964
1965
1966
1967
1968
1969
1970
1971
1972
1973
1974
1975
1976
1977
1978
1979
1980
1981
1982
1983
1984
1985
1986
1987
1988
1989
1990
1991
1992
1993
1994
1995
1996
1997
1998
1999
2000
2001
2002
2003
2004
2005
2006

For the speakers in this study, it is not only the lag between coronal and dorsal gestures that differs systematically between liquids, but also the relative lag between the dorsal gestures of the vowel and liquid. At both syllable margins, TB–V duration is longer for rhotics than laterals, and it constitutes a greater proportion of the total articulatory duration (TT–V) compared to the longer laterals. It is possible that the longer mean transition between the vowel target and the dorsal target of the following rhotic is related to the greater exertion of coarticulatory dominance by rhotics if the production of rhotics is controlled to reduce the potential for articulatory interaction with adjacent vowels. In a gestural representation, this could possibly be understood in terms of minimizing temporal overlap between a vowel and the dorsal gesture of a coda liquid with a high blending strength specification.

Vowel quality could be expected to interact with TB–V duration in such a way that a longer mean transition is expected in rimes with vowels for which the tongue body gesture is more incompatible with that of the liquid. This is borne out in our data in rimes with laterals. A linear mixed model was constructed to examine the effect of vowel quality on TB–V lag in lateral codas. TB–V lag was modelled as a function of vowel backness with random intercepts for speaker (details in Table B6). Front vowels [i-ɪ-eɪ-ɛ-æ] had a greater effect on TB–V lag than back vowels [ʌ-ɑ-oʊ-ʊ-u], increasing it by 94 ms ($\beta = 94.4$, $t(115) = 8.79$, $p < 0.001$; $d = 1.24$, POWER = 100%). The influence of vowel quality on TB–V lag in coda rhotics cannot be reliably modelled in the same way in these data due to sparsity and imbalance in the equivalent subset of rhotic-final rimes, but this would be valuable to examine in a future study. An important consideration for this type of analysis is what constitutes a ‘compatible’ tongue body gesture: the data illustrated in Figs. 9, 11, 13 and 15 reveal that even for back vowels, different vowel qualities map more closely onto the rhotic postures produced by different speakers at the dorsal target; for laterals, on the other hand, it is largely backness that appears to distinguish vowels that are matched with the dorsal posture of liquid (Figs. 8, 10, 12 and 14).

Collectively, these data suggest that laterals may have a greater adaptability in the ways that they can combine with vowels compared to rhotics. Overall, according to these methods of comparison of tongue shape and intergestural timing, the laterals produced by these speakers exert less dominance on the vowels they coarticulate with, and it is possible that lingual gestures in a lateral may be more independent. Both of these properties may allow the lateral greater freedom to combine phonotactically with a wider range of segments than rhotics, including those with gestures specified for goals which differ from those of the liquid.

4.7. Implications for Models of Syllable Structure

These data raise some important questions about gestural organization in syllables, and coordination in syllable rimes in particular. Pouplier (2012) and Brunner et al. (2014) have proposed that timing relationships between a consonant and tautosyllabic vowel depend on the coarticulatory properties of the consonant. Evidence for this was provided by an EMA analysis of Polish onset cluster production (Pastätter & Pou-

2007
2008
2009
2010
2011
2012
2013
2014
2015
2016
2017
2018
2019
2020
2021
2022
2023
2024
2025
plier, 2017), which revealed that sibilants and alveolar sonorants show less overlap with a following vowel compared to labials, consistent with the hypothesis that the degree of overlap in a CV sequence is a function of the intrinsic coarticulatory resistance of the consonant. This proposal is consistent with our finding that the consonant exhibiting the greater stability against coarticulatory influence from vowels – the rhotic – shows a greater mean lag between the achievement of its tongue body gesture and that of the preceding vowel (Fig. 20). A greater lag could be interpreted as an indirect measure of less gestural overlap, because it indicates a greater duration between achievement of gestural targets, suggesting there is less dorsal overlap in a rhotic-final rime. On the other hand, if the TT–TB lag is also considered, the lags in Fig. 20 suggest that the liquid characterized by lower coarticulatory resistance according to the rtMRI analysis – the lateral – shows less *overall* overlap with the preceding vowel in a rime.

2026
2027
2028
2029
2030
2031
2032
2033
2034
2035
2036
2037
2038
2039
2040
2041
2042
There are important differences between this study and that of Pastätter & Pouplier (2017). Most critically, their study examined complex onsets – which are hypothesized to be in a synchronous relationship with the tautosyllabic vowel – while we focused on simplex codas, which are assumed to be coupled asynchronously to the preceding vowel (Browman & Goldstein, 1992). Coarticulatory influences on temporal displacement around the C-center in a syllable onset (Browman & Goldstein, 1988) might differ in important ways from temporal reorganization in an anti-phase coda. Furthermore, the English liquids compared in this study both consist of tongue body gestures, while Pastätter & Pouplier (2017) examined Polish labials, coronals, nasals, and a clear lateral, none of which may have a strong dorsal component (although see Proctor, 2011, on tongue body control in clear Spanish laterals). Although the relative coarticulatory properties of consonants have been examined in detail in Catalan and some other languages (Recasens, 1984; Recasens & Espinosa, 2009; Recasens & Rodríguez, 2017, etc.), more work is required to understand how consonants specified for a tongue body gesture interact with adjacent segments in English.

2043
2044
2045
2046
2047
2048
2049
2050
2051
2052
2053
2054
2055
2056
2057
2058
2059
2060
The principles governing temporal organization in codas are still an active area of research. Data showing sequential organization of post-vocalic gestures in some languages is consistent with models in which coda segments are coupled anti-phase to the nucleus (Krakow, 1999; Browman & Goldstein, 1995b), but studies of coda clusters and multi-gestural segments reveal some more complex patterns of coordination in codas, which have given rise to alternative models (Marin & Pouplier, 2010; Marin, 2013; Tilsen, 2016, etc.). The intergestural timing patterns revealed by these rtMRI data are broadly consistent with models of other multi-gestural segments in which a lingual gesture is coupled anti-phase with the nucleus, and a secondary gesture is coupled to that linking gesture – a model which has been used to account for timing patterns in English nasal codas (Byrd et al., 2009). Yet liquids present a more complicated case in some respects than nasals, as the two primary constituent gestures are both lingual, raising the question of which gesture in a coda liquid would be coupled to a preceding vowel. Because intergestural timing in American English coda liquids broadly patterns with coda nasals, they could possibly be modelled as having the coronal gesture coupled anti-phase to the vowel (Byrd et al., 2009) – a model considered in more detail in Walker & Proctor

2066
2067
2068
2069
2070
2071 (in press). Marin & Pouplier (2010) compare evidence for different models of organization of coda laterals,
2072 including direct coupling of both lingual gestures to the preceding vowel. It remains an open question
2073 whether the different TB–TT lags observed between the liquids in this study arise from different additional
2074 coupling relationships or whether they are due to other intrinsic properties of each type of liquid, such as
2075 differences in constriction location or the formation of a side branch in the lateral. A related issue is whether
2076 principles of recoverability play into gestural organization (Byrd, 1996; Chitoran et al., 2002). More data
2077 obtained with greater temporal resolution from a greater number of speakers will be required to shed more
2078 light on these possibilities and to further investigate the influence of vowel quality on timing patterns.
2079
2080
2081
2082

2083 *4.8. Further Considerations*

2084

2085 The data presented in this study are limited in some important respects. There are many more factors
2086 that have been shown to influence liquid production which could not be controlled or modelled in these data.
2087 In particular, lexical and morphological factors can influence liquid behaviour at a sub-segmental level, which
2088 may affect the way that these consonants interact with other elements in the rime. For example, Lin et al.
2089 (2014) found that word frequency has a greater effect on coronal articulation of American English laterals
2090 (more lenition in high-frequency words) than on the dorsal gesture, which remains relatively stable. Lee-Kim
2091 et al. (2013) showed that stem-final word medial laterals (e.g. ‘*tall-est*’) are not as dark as word- and stem-
2092 final allophones (‘*tall*’) in American English. Ultrasound data revealed that the most consistent articulatory
2093 correlate of lateral darkness for the speakers in that study of was tongue body lowering, which suggests that
2094 coda laterals might coarticulate differently with preceding vowels depending on the morphological context,
2095 as well as intrinsic coarticulatory blending factors.
2096
2097
2098
2099

2100 *4.9. Future Directions*

2101

2102 More detailed phonetic characterization of coda liquids and the ways that they interact with different
2103 vowels will require information about articulation beyond the mid-sagittal plane. The use of parasagittal
2104 sensors in EMA analysis is providing new insights into the way that the sides of the tongue are coordinated
2105 with coronal and dorsal activity in the midsagittal plane (Ying et al., 2017), and new 3d rtMRI methods
2106 will offer further advantages in parasagittal sensing (e.g. Zhu et al., 2013).
2107
2108

2109 The default video reconstruction frame rate of these rtMRI data is not rapid enough to resolve some
2110 fine timing details of gestural coordination, especially near-synchronous articulatory activity. Although
2111 temporal resolution could be improved in the existing data using alternative video reconstruction techniques
2112 (e.g. Proctor et al., 2015), future studies of intergestural timing and coarticulation in liquids will be better
2113 served by new rtMRI sequences offering greater temporal and spatial resolution (e.g. Lingala et al., 2017).
2114
2115

2116 This study has identified some patterns of coarticulation and intergestural timing which might arise from
2117 hypothesized differences in blending strength in the gestural representation of liquids. A more complete
2118
2119
2120
2121
2122
2123
2124

2125
2126
2127
2128
2129
2130
2131
2132
2133
2134
2135
2136
2137
2138
2139
2140
2141
2142
2143
2144
2145
2146
2147
2148
2149
2150
2151
2152
2153
2154
2155
2156
2157
2158
2159
2160
2161
2162
2163
2164
2165
2166
2167
2168
2169
2170
2171
2172
2173
2174
2175
2176
2177
2178
2179
2180
2181
2182
2183

understanding of the specified blending strength of English liquid consonants and the dynamics of their interactions with vowels will require more data about tongue shaping and gestural timing in vowel-liquid rimes produced by more speakers, as well as modelling. TADA – an implementation of the Task Dynamic model of inter-articulator coordination in speech (Nam et al., 2004) – allows manipulation of constriction location and degree, and blending strength specifications for the gestures in an utterance, and simulation of the resulting articulatory dynamics (Nam et al., 2006). It is beyond the scope of the current study to model the effects of blending strength and vowel quality on liquid interactions with adjacent vowels, but these parameters should be systematically manipulated in a series of TADA simulations to test these ideas further.

2184
2185
2186
2187
2188
2189
2190
2191
2192
2193
2194
2195
2196
2197
2198
2199
2200
2201
2202
2203
2204
2205
2206
2207
2208
2209
2210
2211
2212
2213
2214
2215
2216
2217
2218
2219
2220
2221
2222
2223
2224
2225
2226
2227
2228
2229
2230
2231
2232
2233
2234
2235
2236
2237
2238
2239
2240
2241
2242

⁷⁹⁰ **Acknowledgments**

This work was supported by National Institutes of Health grant NIH Grant R01 DC007124; and Australian Research Council Award DE150100318. We are grateful to Taehong Cho and three anonymous reviewers for their comments on earlier drafts of this manuscript.

Appendix A. Summary of Statistical Modeling: Rhotic Labial Articulation

Statistics of linear mixed-effects models examining the effect of consonant type on labial articulation (Sec. 3.2) are summarised in Tables A1 and A2. Position coding: Coda = 0, Onset = 1. p -values are calculated with the *lmerTest* package (Kuznetsova et al., 2017) using Satterthwaite’s method of approximation.

Table A1: **Rhotic Labial Aperture (mm)** as a function of Syllable Position.

| MODEL: $LA \sim Pos + (1 Subj)$ | | | | | |
|--|-------------|----------|-------|---------|----------|
| RANDOM EFFECTS: | | | | | |
| Groups | Name | Variance | S.D. | | |
| Subj | (Intercept) | 12.53 | 3.54 | | |
| Residual | | 9.20 | 3.03 | | |
| Number of observations: 168, groups: Subj, 4 | | | | | |
| FIXED EFFECTS: | | | | | |
| | Estimate | SE | df | t-value | Pr(> t) |
| (Intercept) | 14.90 | 1.81 | 3.2 | 8.22 | 0.003 |
| Pos-Ons | -9.17 | 0.49 | 163.0 | -18.77 | < 2e-16 |

Table A2: **Rhotic Labial Protrusion (mm)** as a function of Syllable Position.

| MODEL: $LP \sim Pos + (1 Subj)$ | | | | | |
|--|-------------|----------|-------|---------|----------|
| RANDOM EFFECTS: | | | | | |
| Groups | Name | Variance | S.D. | | |
| Subj | (Intercept) | 13.3 | 3.7 | | |
| Residual | | 9.0 | 3.0 | | |
| Number of observations: 168, groups: Subj, 4 | | | | | |
| FIXED EFFECTS: | | | | | |
| | Estimate | SE | df | t-value | Pr(> t) |
| (Intercept) | 1.55 | 1.87 | 3.2 | 0.83 | 0.464 |
| Pos-Ons | 5.65 | 0.49 | 163.0 | 11.72 | < 2e-16 |

2302
2303
2304
2305
2306
2307 **Appendix B. Summary of Statistical Modeling: Intergestural Timing**
2308

2309 Statistics of linear mixed-effects models examining the effect of consonant type on intergestural timing
2310 relationships (Sec. 3.3) are summarised in Tables B1 to B5. Consonant coding used in all models: Lateral = 0
2311 800 (Intercept), Rhotic = 1. *p*-values are calculated with the *lmerTest* package (Kuznetsova et al., 2017) using
2312 Satterthwaite’s method of approximation.
2313
2314

2315
2316 Table B1: **TT–V lag (ms) in Onsets**
2317

2318 RANDOM EFFECTS:

| Groups | Name | Variance | S.D. |
|----------|-------------|----------|------|
| Subj | (Intercept) | 124.6 | 11.3 |
| Residual | | 2495.7 | 50.0 |

2319
2320
2321
2322
2323
2324 Number of observations: 228, groups: Subj, 4
2325

2326 FIXED EFFECTS:

| | Estimate | SE | df | t value | Pr(> t) |
|-------------|----------|-----|-------|---------|----------|
| (Intercept) | -274.1 | 7.2 | 4.6 | -38.0 | 6.9e-07 |
| Cons-Rhotic | 66.1 | 6.6 | 223.0 | 10.0 | < 2e-16 |

2327
2328
2329
2330
2331
2332

2333 Table B2: **TB–V lag (ms) in Onsets**
2334

2335 RANDOM EFFECTS:

| Groups | Name | Variance | S.D. |
|----------|-------------|----------|------|
| Subj | (Intercept) | 59.6 | 7.7 |
| Residual | | 2375.9 | 48.7 |

2336
2337
2338
2339
2340
2341
2342 Number of observations: 228, groups: Subj, 4
2343

2344 FIXED EFFECTS:

| | Estimate | SE | df | t value | Pr(> t) |
|-------------|----------|-----|-------|---------|----------|
| (Intercept) | -187.5 | 5.9 | 5.6 | -31.8 | 1.44e-07 |
| Cons-Rhotic | -20.5 | 6.5 | 223.0 | -3.2 | 0.0018 |

2345
2346
2347
2348
2349
2350
2351
2352
2353
2354
2355
2356
2357
2358
2359
2360

2361
2362
2363
2364
2365
2366
2367
2368
2369
2370
2371
2372
2373
2374
2375
2376
2377
2378
2379
2380
2381
2382
2383
2384
2385
2386
2387
2388
2389
2390
2391
2392
2393
2394
2395
2396
2397
2398
2399
2400
2401
2402
2403
2404
2405
2406
2407
2408
2409
2410
2411
2412
2413
2414
2415
2416
2417
2418
2419

Table B3: **TT-V lag (ms) in Codas**

RANDOM EFFECTS:

| Groups | Name | Variance | S.D. |
|----------|-------------|----------|------|
| Subj | (Intercept) | 7040 | 83.9 |
| Residual | | 4167 | 64.6 |

Number of observations: 180, groups: Subj, 4

FIXED EFFECTS:

| | Estimate | SE | df | t value | Pr(> t) |
|-------------|----------|------|-------|---------|----------|
| (Intercept) | 343.4 | 42.4 | 3.0 | 8.1 | 0.0037 |
| Cons-Rhotic | -44.3 | 10.2 | 175.0 | -4.3 | 2.45e-05 |

Table B4: **TB-V lag (ms) in Codas**

RANDOM EFFECTS:

| Groups | Name | Variance | S.D. |
|----------|-------------|----------|------|
| Subj | (Intercept) | 1766 | 42.0 |
| Residual | | 4608 | 67.9 |

Number of observations: 180, groups: Subj, 4

FIXED EFFECTS:

| | Estimate | SE | df | t value | Pr(> t) |
|-------------|----------|------|-------|---------|----------|
| (Intercept) | 195.3 | 21.9 | 3.2 | 8.9 | 0.0024 |
| Cons-Rhotic | 25.7 | 10.7 | 175.0 | 2.4 | 0.0176 |

Table B5: **TT-TB lag (ms) in Codas**

RANDOM EFFECTS:

| Groups | Name | Variance | S.D. |
|----------|-------------|----------|------|
| Subj | (Intercept) | 3166 | 56.3 |
| Residual | | 3201 | 56.6 |

Number of observations: 180, groups: Subj, 4

FIXED EFFECTS:

| | Estimate | SE | df | t value | Pr(> t) |
|-------------|----------|------|-------|---------|----------|
| (Intercept) | 148.1 | 28.6 | 3.1 | 5.2 | 0.0133 |
| Cons-Rhotic | -70.0 | 8.9 | 175.0 | -7.8 | 4.73e-13 |

2420
 2421
 2422
 2423
 2424
 2425
 2426
 2427
 2428
 2429
 2430
 2431
 2432
 2433
 2434
 2435
 2436
 2437
 2438
 2439
 2440
 2441
 2442
 2443
 2444
 2445
 2446
 2447
 2448
 2449
 2450
 2451
 2452
 2453
 2454
 2455
 2456
 2457
 2458
 2459
 2460
 2461
 2462
 2463
 2464
 2465
 2466
 2467
 2468
 2469
 2470
 2471
 2472
 2473
 2474
 2475
 2476
 2477
 2478

Table B6: **TB–V lag (ms) in Lateral Codas as a function of Vowel Backness.**

Vowel quality treatment coded as BACK [Λ - α - $\text{o}\ddot{\text{u}}$ - v - u] = 0; FRONT [i - i - e - e - æ] = 1.

RANDOM EFFECTS:

| Groups | Name | Variance | S.D. |
|----------|-------------|----------|------|
| Subj | (Intercept) | 2360 | 48.6 |
| Residual | | 3457 | 58.8 |

Number of observations: 120, groups: Subj, 4

FIXED EFFECTS:

| | Estimate | SE | df | t value | Pr(> t) |
|-------------|----------|------|-------|---------|----------|
| (Intercept) | 148.1 | 25.5 | 3.3 | 5.8 | 0.0078 |
| Vfb-Front | 94.4 | 10.7 | 115.0 | 8.8 | 1.66e-14 |

Appendix C. Summary of Statistical Modeling: Vowel–Liquid Coarticulatory Interaction

Statistics of linear mixed-effects models examining the effects of consonant type and syllable position on lingual displacement (Sec. 3.5) are summarised in Tables C1 and C2. Consonant coding: Lateral = 0, Rhotic = 1. Position coding: Coda = 0, Onset = 1. p -values are calculated with the *lmerTest* package (Kuznetsova et al., 2017) using Satterthwaite’s method of approximation.

Table C1: **Coarticulatory Resistance**: log lingual displacement of liquids (mm/gridline) as a function of Consonant type (Lat/Rho) and syllable Position (Coda/Ons).

MODEL: $\log(Dist) \sim Con * Pos + (Con|Subj) + (Pos|Subj)$

RANDOM EFFECTS:

| Groups | Name | Variance | S.D. | Corr |
|----------|-------------|----------|-------|-------|
| Subj | (Intercept) | 0.007 | 0.081 | |
| | Con-Rho | 0.052 | 0.228 | -0.61 |
| Subj.1 | (Intercept) | 0.021 | 0.142 | |
| | Pos-Ons | 0.098 | 0.313 | -0.69 |
| Residual | | 0.093 | 0.304 | |

Number of observations: 480, groups: Subj, 4

FIXED EFFECTS:

| | Estimate | SE | df | t-value | Pr(> t) |
|------------------|----------|-------|--------|---------|----------|
| (Intercept) | 0.646 | 0.086 | 2.01 | 7.47 | 0.0172 |
| Con-Rho | -0.407 | 0.121 | 3.35 | -3.37 | 0.0368 |
| Pos-Ons | -0.178 | 0.161 | 3.19 | -1.11 | 0.3452 |
| Con-Rho:Pos-Coda | 0.188 | 0.056 | 467.00 | -3.39 | 0.0008 |

CORRELATION OF FIXED EFFECTS:

| | (Intr) | Con-Rho | Pos-Ons |
|-----------------|--------|---------|---------|
| Con-Rho | -0.343 | | |
| Pos-Ons | -0.606 | 0.040 | |
| Con-Rho:Pos-Ons | 0.161 | -0.230 | -0.172 |

2538
 2539
 2540
 2541
 2542
 2543
 2544
 2545
 2546
 2547
 2548
 2549
 2550
 2551
 2552
 2553
 2554
 2555
 2556
 2557
 2558
 2559
 2560
 2561
 2562
 2563
 2564
 2565
 2566
 2567
 2568
 2569
 2570
 2571
 2572
 2573
 2574
 2575
 2576
 2577
 2578
 2579
 2580
 2581
 2582
 2583
 2584
 2585
 2586
 2587
 2588
 2589
 2590
 2591
 2592
 2593
 2594
 2595
 2596

Table C2: **Coarticulatory Aggression**: lingual displacement of vowels (mm/gridline) as a function of Consonant type (Lat/Rho) and syllable Position (Coda/Ons).

MODEL: $Dist \sim Con * Pos + (Pos|Subj)$

RANDOM EFFECTS:

| Groups | Name | Variance | S.D. | Corr |
|----------|-------------|----------|-------|-------|
| Subj | (Intercept) | 0.035 | 0.187 | |
| | Pos-Ons | 0.048 | 0.218 | -0.95 |
| Residual | | 0.061 | 0.248 | |

Number of observations: 80, groups: Subj, 4

FIXED EFFECTS:

| | Estimate | SE | df | t-value | Pr(> t) |
|-----------------|----------|-------|-------|---------|----------|
| (Intercept) | 0.581 | 0.109 | 3.96 | 5.35 | 0.0061 |
| Con-Rho | 0.292 | 0.078 | 70.00 | 3.73 | 0.0004 |
| Pos-Ons | 0.049 | 0.134 | 4.35 | 0.37 | 0.7321 |
| Con-Rho:Pos-Ons | -0.220 | 0.111 | 70.00 | -1.99 | 0.0508 |

CORRELATION OF FIXED EFFECTS:

| | (Intr) | Con-Rho | Pos-Ons |
|-----------------|--------|---------|---------|
| Con-Rho | -0.360 | | |
| Pos-Ons | -0.877 | 0.292 | |
| Con-Rho:Pos-Ons | 0.225 | -0.707 | -0.412 |

References

- Alwan, A., Narayanan, S., & Haker, K. (1997). Toward articulatory-acoustic models for liquid approximants based on MRI and EPG data. Part II. The rhotics. *J. Acoust. Soc. Am.*, *101*, 1078–1089.
- Bates, D., Mächler, M., Bolker, B., & Walker, S. (2015). Fitting linear mixed-effects models using lme4. *Journal of Statistical Software*, *667*, 1–48.
- Bladon, R. A. W., & Al Bamerni, A. (1976). Coarticulation resistance in English /l/. *Journal of Phonetics*, *4*, 137–150.
- Bresch, E., Kim, Y.-C., Nayak, K., Byrd, D., & Narayanan, S. (2008). Seeing speech: Capturing vocal tract shaping using real-time magnetic resonance imaging [Exploratory DSP]. *IEEE Signal Process. Mag.*, *25*, 123–132.
- Bresch, E., Nielsen, J., Nayak, K., & Narayanan, S. (2006). Synchronized and noise-robust audio recordings during realtime magnetic resonance imaging scans. *J. Acoust. Soc. Am.*, *120*, 1791–1794.
- Browman, C. P., & Goldstein, L. (1988). Some notes on syllable structure in articulatory phonology. *Phonetica*, *45*, 140–155.
- Browman, C. P., & Goldstein, L. (1995a). Dynamics and articulatory phonology. In T. van Gelder, & B. Port (Eds.), *Mind as motion: Explorations in the dynamics of cognition* (pp. 175–193). Cambridge, MA: MIT Press.
- Browman, C. P., & Goldstein, L. M. (1986). Towards an articulatory phonology. *Phonology Yearbook*, *3*, 219–252.
- Browman, C. P., & Goldstein, L. M. (1989). Articulatory gestures as phonological units. *Phonology*, *6*, 201–251.
- Browman, C. P., & Goldstein, L. M. (1992). Articulatory phonology: an overview. *Phonetica*, *49*, 155–180.
- Browman, C. P., & Goldstein, L. M. (1995b). Gestural syllable position effects in American English. In F. Bell-Berti, & L. J. Raphael (Eds.), *Producing speech: contemporary issues (for Katherine Safford Harris)* (pp. 19–34). New York: AIP Press.
- Brunner, J., Geng, C., Sotiropoulou, S., & Gafos, A. (2014). Timing of german onset and word boundary clusters. *Laboratory Phonology*, *5*, 403–454.
- Brysbaert, M., & Stevens, M. (2018). Power analysis and effect size in mixed effects models: A tutorial. *Journal of Cognition*, *1*, 1–20.
- Byrd, D. (1996). Influences on articulatory timing in consonant sequences. *Journal of Phonetics*, *24*, 209–244.
- Byrd, D., Tobin, S., Bresch, E., & Narayanan, S. (2009). Timing effects of syllable structure and stress on nasals: a real-time MRI examination. *Journal of Phonetics*, *37*, 97–110.
- Chitoran, I., Goldstein, L. M., & Byrd, D. (2002). Gestural overlap and recoverability: Articulatory evidence from Georgian. In C. Gussenhoven, & N. Warner (Eds.), *Laboratory phonology 7* (pp. 419–447). Berlin; New York: Mouton de Gruyter.
- Delattre, P., & Freeman, D. C. (1968). A dialect study of American r's by x-ray motion picture. *Linguistics*, *44*, 29–68.
- Espy-Wilson, C. Y., Boyce, S. E., Jackson, M., Narayanan, S., & Alwan, A. (2000). Acoustic modeling of American English /r/. *J. Acoust. Soc. Am.*, *108*, 343–356.
- Farnetani, E. (1990). Vcv lingual coarticulation and its spatiotemporal domain. In W. Hardcastle, & A. Marchal (Eds.), *Speech production and speech modelling* (pp. 93–130). Springer.
- Fowler, C. A., & Saltzman, E. (1993). Coordination and coarticulation in speech production. *Language and Speech*, *36*, 171–195.
- Gick, B. (2003). Articulatory correlates of ambisyllabicity in English glides and liquids. In J. Local, R. Ogden, & R. A. M. Temple (Eds.), *Papers in laboratory phonology VI: Phonetic interpretation* (pp. 222–236). Cambridge; New York: Cambridge University Press.
- Gick, B., & Campbell, F. (2003). Intergestural timing in English /r/. In *Proc. 15th Intl. Congress of Phonetic Sciences* (pp. 1911–1914). ICPHS.
- Gick, B., Campbell, F., Oh, S., & Tamburri-Watt, L. (2006). Toward universals in the gestural organization of syllables: A cross-linguistic study of liquids. *Journal of Phonetics*, *34*, 49–72.
- Gick, B., Iskarous, K., Whalen, D. H., & Goldstein, L. M. (2003). Constraints on variations in the production of English /r/. In *6th International Seminar on Speech Production* (pp. 73–78). Sydney: ISSP.

- 2656
2657
2658
2659
2660
2661 Giegerich, H. J. (1992). *English phonology: An introduction*. Cambridge Univ. Press.
- 2662 Giles, S. B., & Moll, K. L. (1975). Cinefluorographic study of selected allophones of English /l/. *Phonetica*, 31, 206–227.
- 2663 Green, P., & MacLeod, C. J. (2016). SIMR: an R package for power analysis of generalized linear mixed models by simulation.
- 2664 *Methods in Ecology and Evolution*, 7, 493–498.
- 2665 855 Hagiwara, R. (1994). Three types of American /r/. *UCLA Working Papers in Phonetics*, (pp. 55–62).
- 2667 Hammond, M. (1999). *The phonology of English: a prosodic optimality-theoretic approach*. Oxford; New York: Oxford
- 2668 Univ. Press.
- 2669 Hardcastle, W. J., & Barry, W. (1989). Articulatory and perceptual factors in /l/ vocalisations in english. *Journal of the*
- 2670 *International Phonetic Association*, 15, 3–17.
- 2671 860 Kenyon, J. S., & Knott, T. A. (1953). *A pronouncing dictionary of American English*. Merriam Springfield, Mass.
- 2672 Kirby, J., & Sonderegger, M. (2018). Mixed-effects design analysis for experimental phonetics. *Journal of Phonetics*, 70, 70–85.
- 2673 Krakow, R. A. (1999). Physiological organization of syllables: a review. *Journal of Phonetics*, 27, 23–54.
- 2674 Kuznetsova, A., Brockhoff, P. B., & Christensen, R. H. B. (2017). lmerTest package: tests in linear mixed effects models.
- 2675 *Journal of Statistical Software*, 82, 1–26.
- 2676 865 Labov, W., Ash, S., & Boberg, C. (2005). *The atlas of North American English: Phonetics, phonology and sound change*.
- 2678 Walter de Gruyter.
- 2679 Lee-Kim, S.-I., Davidson, L., & Hwang, S. (2013). Morphological effects on the darkness of English intervocalic /l/. *Laboratory*
- 2680 *Phonology*, 4, 475–511.
- 2681 Leidner, D. R. (1976). The articulation of American English /l/: A study of gestural synergy and antagonism. *Journal of*
- 2682 870 *Phonetics*, 4, 327–335.
- 2683 Lin, S., Davies, B., Turpin, M., Ross, A., & Demuth, K. (2014). The Articulation of Kaytetye Coronals. In *Proc. 14th Conf. on*
- 2684 *Laboratory Phonology*. National Institute for Japanese Linguistics Tokyo: NINJAL.
- 2685 Lindau, M. (1985). The story of /r/. In V. Fromkin (Ed.), *Phonetic Linguistics: Essays in Honor of Peter Ladefoged* (pp.
- 2686 157–168). Orlando: Academic Press.
- 2687 875 Lingala, S. G., Zhu, Y., Kim, Y.-C., Toutios, A., Narayanan, S., & Nayak, K. S. (2017). A fast and flexible MRI system for
- 2688 the study of dynamic vocal tract shaping. *Magnetic Resonance in Medicine*, 77, 112–125.
- 2689 Marin, S. (2013). The temporal organization of complex onsets and codas in Romanian: a gestural approach. *Journal of*
- 2690 *Phonetics*, 41, 211 – 227.
- 2691 Marin, S., & Pouplier, M. (2010). Temporal organization of complex onsets and codas in american english: Testing the
- 2692 880 predictions of a gestural coupling model. *Motor Control*, 14, 380–407.
- 2693 Mielke, J., Baker, A., & Archangeli, D. (2016). Individual-level contact limits phonological complexity: Evidence from bunched
- 2694 and retroflex /r/. *Language*, 92, 101–140.
- 2695 Nam, H., Goldstein, L., Browman, C., Rubin, P., Proctor, M., & Saltzman, E. (2006). Tada (task dynamics application)
- 2696 manual.
- 2697 885 Nam, H., Goldstein, L., Saltzman, E., & Byrd, D. (2004). Tada: An enhanced, portable task dynamics model in matlab.
- 2699 *J. Acoust. Soc. Am.*, 115, 2430. URL: <http://adsabs.harvard.edu/abs/2001ASAJ...115.2430N>.
- 2700 Nam, H., Goldstein, L. M., & Saltzman, E. L. (2009). Self-organization of syllable structure: A coupled oscillator model. In
- 2701 I. Chitoran, C. Coupé, E. Marisco, & F. Pellegrino (Eds.), *Approaches to Phonological Complexity* (pp. 299–328). Berlin:
- 2702 Mouton.
- 2703 890 Narayanan, S., Nayak, K., Lee, S., Sethy, A., & Byrd, D. (2004). An approach to real-time magnetic resonance imaging for
- 2704 speech production. *J. Acoust. Soc. Am.*, 115, 1771–1776.
- 2705 Narayanan, S., Toutios, A., Ramanarayanan, V., Lammert, A., Kim, J., Lee, S., Nayak, K., Kim, Y.-C., Zhu, Y., Goldstein,
- 2706 L., Byrd, D., Bresch, E., Ghosh, P., Katsamanis, A., & Proctor, M. (2014). Real-time magnetic resonance imaging and
- 2707
- 2708
- 2709
- 2710
- 2711
- 2712
- 2713
- 2714

- 2715 electromagnetic articuography database for speech production research (TC). *J. Acoust. Soc. Am.*, 136, 1307–1311.
- 2716
- 2717
- 2718
- 2719
- 2720
- 2721
- 2722 895 Narayanan, S. S., Alwan, A. A., & Haker, K. (1997). Toward articulatory-acoustic models for liquid approximants based on
MRI and EPG data. Part I. The laterals. *J. Acoust. Soc. Am.*, 101, 1064–1077.
- 2723
- 2724 Pastätter, M., & Pouplier, M. (2017). Articulatory mechanisms underlying onset-vowel organization. *Journal of Phonetics*,
2725 65, 1 – 14.
- 2726
- 2727 Pouplier, M. (2012). The gestural approach to syllable structure: Universal, language-and cluster-specific aspects. In S. Fuchs,
2728 900 M. Weirich, D. Pape, & P. Perrier (Eds.), *Speech planning and dynamics* (pp. 63–96). Peter Lang Verlag Frankfurt am
Main.
- 2729
- 2730 Proctor, M. (2011). Towards a gestural characterization of liquids: Evidence from Spanish and Russian. *Laboratory Phonology*,
2731 2, 451–485.
- 2732
- 2733 Proctor, M., Lo, C., & Narayanan, S. (2015). Articulation of English Vowels in Running Speech: a Real-time MRI Study. In
2734 905 *Proc. Int'l Congress on Phonetic Sciences*. Glasgow.
- 2735
- 2736 Proctor, M., & Walker, R. (2012). Articulatory bases of English liquids. In S. Parker (Ed.), *The Sonority Controversy* (pp.
2737 285–312). Berlin: De Gruyter volume 18 of *Studies in Generative Grammar*.
- 2738
- 2739 Proctor, M. I., Bone, D., & Narayanan, S. S. (2010). Rapid semi-automatic segmentation of real-time Magnetic Resonance
2740 Images for parametric vocal tract analysis. In *Proc. Int'l Conf. on Speech Communication and Technology* (pp. 1576–1579).
2741 910 Makuhari, Japan.
- 2742
- 2743 Proctor, M. I., Katsamanis, N., Goldstein, L., Hagedorn, C., Lammert, A., & Narayanan, S. (2011). Direct estimation of
2744 articulatory dynamics from real-time Magnetic Resonance Image sequences. In *Proc. Int'l Conf. on Speech Communication
2745 and Technology* (pp. 281–284). Florence, Italy.
- 2746
- 2747 R Core Team (2018). *R: A Language and Environment for Statistical Computing*. R Foundation for Statistical Computing
2748 915 Vienna, Austria. URL: <https://www.R-project.org/>.
- 2749
- 2750 Recasens, D. (1984). V-to-C Coarticulation in Catalan VCV Sequences: An Articulatory and Acoustical Study. *Journal of
2751 Phonetics*, 12, 61–73.
- 2752
- 2753 Recasens, D., & Espinosa, A. (2009). An articulatory investigation of lingual coarticulatory resistance and aggressiveness for
2754 consonants and vowels in Catalan. *J. Acoust. Soc. Am.*, 125, 2288–2298.
- 2755
- 2756 920 Recasens, D., Pallarès, M. D., & Fontdevila, J. (1997). A model of lingual coarticulation based on articulatory constraints.
J. Acoust. Soc. Am., 102, 544–561.
- 2757
- 2758 Recasens, D., & Rodríguez, C. (2016). A study on coarticulatory resistance and aggressiveness for front lingual consonants and
2759 vowels using ultrasound. *Journal of Phonetics*, 59, 58–75.
- 2760
- 2761 Recasens, D., & Rodríguez, C. (2017). Lingual Articulation and Coarticulation for Catalan Consonants and Vowels: An
2762 925 Ultrasound Study. *Phonetica*, 74, 125–156.
- 2763
- 2764 Saltzman, E. L., & Munhall, K. G. (1989). A dynamical approach to gestural patterning in speech production. *Ecological
2765 Psychology*, 1, 333–382.
- 2766
- 2767 Saltzman, E. L., Rubin, P. E., Goldstein, L., & Browman, C. P. (1987). Task-dynamic modeling of interarticulator coordination.
2768 *J. Acoust. Soc. Am.*, 82, S15.
- 2769
- 2770 930 Scobbie, J. M., & Pouplier, M. (2010). The role of syllable structure in external sandhi: An EPG study of vocalisation and
retraction in word-final English /l/. *Journal of Phonetics*, 38, 240–259.
- 2771
- 2772 Sproat, R., & Fujimura, O. (1993). Allophonic variation in English /l/ and its implications for phonetic implementation.
2773 *Journal of Phonetics*, 21, 291–311.
- 2774
- 2775 Tilsen, S. (2016). Selection and coordination: The articulatory basis for the emergence of phonological structure. *Journal of
2776 Phonetics*, 55, 53–77.
- 2777
- 2778 Uldall, E. T. (1958). American 'molar' r and 'flapped' r. *Revista do Laboratorio de Fone'tica Experimental (Coimbra)*, 4,

2774
2775
2776
2777
2778
2779
2780
2781
2782
2783
2784
2785
2786
2787
2788
2789
2790
2791
2792
2793
2794
2795
2796
2797
2798
2799
2800
2801
2802
2803
2804
2805
2806
2807
2808
2809
2810
2811
2812
2813
2814
2815
2816
2817
2818
2819
2820
2821
2822
2823
2824
2825
2826
2827
2828
2829
2830
2831
2832

103–106.

Walker, R., & Proctor, M. (2013). Articulatory overlap in English syllables with postvocalic /ɹ/. *Proceedings of Meetings on Acoustics*, 19, 060259.

940 Walker, R., & Proctor, M. I. (in press). The Organization and Structure of Rhotics in American English Rimes. *Phonology*, 36.

Wells, J. (2008). *Longman pronunciation dictionary*. Pearson Education India.

Wells, J. C. (1982). *Accents of English, vol.1: An Introduction* volume 1. Cambridge: Cambridge Univ. Press.

Westfall, J., Kenny, D. A., & Judd, C. M. (2014). Statistical power and optimal design in experiments in which samples of 945 participants respond to samples of stimuli. *Journal of Experimental Psychology: General*, 143, 2020–2045.

Ying, J., Carignan, C., Shaw, J. A., Proctor, M., Derrick, D., & Best, C. T. (2017). Temporal Dynamics of Lateral Channel Formation in /l/: 3D EMA Data from Australian English. (pp. 2978–2982).

Zawadzki, P. A., & Kuehn, D. P. (1980). A cineradiographic study of static and dynamic aspects of American English /r/. *Phonetica*, 37, 253–266.

950 Zhou, X., Espy-Wilson, C. Y., Boyce, S., Tiede, M., Holland, C., & Choe, A. (2008). A magnetic resonance imaging-based articulatory and acoustic study of ‘retroflex’ and ‘bunched’ American English /r/. *J. Acoust. Soc. Am.*, 123, 4466–4481.

Zhu, Y., Kim, Y.-C., Proctor, M. I., Narayanan, S., & Nayak, K. S. (2013). Dynamic 3D Visualization of Vocal Tract Shaping during Speech. *IEEE Trans. Medical Imaging*, 32, 838–848.